« This training is bound for glory » : selection by experimental evolution of a bacteriophage with expanded host-range and increased virulence

Amandine Maurin[1], Marie Vasse[1], Carlos Zarate-Chaves[2], Cécile Breyton[3], Sarah Bouzidi[1], Juliette Hayer[1], Jacques Dainat[1], Margaux Mesleard-Roux[1], François-Xavier Weill[4], Ignacio G. Bravo[1], Alexandre Feugier[5], Rémy Froissart[1*]

1. MIVEGEC (Univ. Montpellier, CNRS, IRD), Montpellier F-34394, France
2. PHIM (IRD, CIRAD, INRAE), F-34394 Montpellier, France
3. IBS (Univ. Grenoble Alpes, CNRS, CEA), F-38044 Grenoble, France
4. Institut Pasteur, Univ. Paris Cité, « Bactéries pathogènes entériques », Centre National de Référence des Escherichia coli, Shigella et Salmonella, F-75015 Paris, France
5. Bokaworm Research Center, F-30310 Vergèze, France

*Corresponding author

Rémy Froissart,

ORCID ID : 0000-0001-8234-1308

CNRS, UMR 5290 MIVEGEC, 911 Av Agropolis 34394 Montpellier, France

+33 (0)467416372

remy.froissart@cnrs.fr

	mail	ORCID
Amandine Maurin	amandine.maurin@ird.fr	
Marie Vasse	contact@marievasse.eu	0000-0003-4081-6664
Carlos Zarate-Chaves	carlos.zarate-chaves@ird.fr	0000-0002-5588-710X
Cécile Breyton	cecile.breyton@ibs.fr	0000-0002-4382-0434
Sarah Bouzidi	sarah.bouzidi@ird.fr	
Juliette Hayer	juliette.hayer@ird.fr	0000-0003-4899-9637
Jacques Dainat	jacques.dainat@ird.fr	0000-0002-6629-0173
Margaux Mesleard-Roux	margaux.mesleard-roux@etu.umontpellier.fr	
François-Xavier Weill	francois-xavier.weill@pasteur.fr	0000-0001-9941-5799
Nacho Bravo	ignacio.bravo@cnrs.fr	0000-0003-3389-3389
Alexandre Feugier	alexandre.feugier@royalcanin.com	
Rémy Froissart	remy.froissart@cnrs.fr	0000-0001-8234-1308

Highlights

- A *Tequintavirus* was evolved on susceptible and resistant *Salmonella enterica*
- Evolved phage populations harbored expanded host-range and increased virulence
- First adaptive mutations optimized receptor recognition in Long Tail Fiber (LTF)
- Reverse-genetics revealed implication of two LTF mutations in host-range expansion

In Brief

Despite that generalism is predicted to evolve at the cost of lower mean fitness, we experimentally selected phage populations with expanded host-range and increased virulence, demonstrating that generalist phages could be easily and usefully generated for phage therapy efforts. - 39 words - 278 characters

Abstract

Phage host-range expansion is predicted to be at the cost of lower mean fitness. We aimed at following the adaptive walks of a virulent phage (*Tequintavirus*) evolving in a spatially variable environment composed of four susceptible and four resistant strains (*Salmonella enterica enterica* pv Tennessee, sequence types ST5018 and ST319 respectively). We evolved a single ancestor through serial passages on the non-coevolving bacterial strains following Appelmans' protocol and obtained several evolved phage populations with expanded host-range and increased virulence. Phage populations sequencing revealed multiple mutations appearing at the same loci (parallel mutations), notably on exo- and endo-nuclease, dUTPase and caudal proteins. Two parallel mutations present on the long tail fiber gene showed to become fixed within the population before the other parallel mutations. Introduction by reverse-genetics of these two mutations into the ancestral genome expanded host-range but not virulence.

Key words

Salmonella, *Tequintavirus*, biocontrol, bacteriophage, host-range, virulence, adaptation

Introduction

Bacteriophages (i.e. phages) are viruses of bacteria known to strongly impact bacterial population dynamics in all environments where bacteria reside (Dion et al., 2020; Chevallereau et al., 2022) such as ocean (Suttle, 2007; Breitbart, 2012), soil (Roux & Emerson, 2022) or gut (Reyes et al., 2010; Norman et al., 2015; Duerkop et al., 2018). Due to their obligatory parasitic biological cycle, bacteriophages need to infect and replicate within as much as possible bacterial hosts. Since most bacterial communities are diverse at the species and genotypic levels, we would expect that most bacteriophages harbor large host-range (Sant et al., 2021). Strickingly, a lot of bacteriophages harbour a narrow host-spectrum that is that they mostly infect few bacterial species (Koskella & Meaden, 2013; Meaden & Koskella, 2013; Hyman & Abedon, 2010; de Jonge et al., 2019; Bono et al., 2021) or only few genotypes of one species (Allen et al., 2017; Mathieu et al., 2020). The reason why we observe so many specialist bacteriophages is still an open question (Bono et al., 2020) and rely on long-standing fundamental question related to specialisation and the cost of generalism (Woolhouse et al., 2001; Leggett et al., 2013). At the cellular level, antagonistic pleiotropy of adaptive mutations might be responsible for cost of generalism, that is that increase in fitness associated to one mutation in one environment can be delerious in an other environment (Brockhurst et al., 2017; Bono et al., 2020; Duffy et al., 2006; Ferris et al., 2007).

Several studies on different phage-bacteria interactions did evaluate the effect of mutations involved in host-range expansion. For instance, by combining several experiments studying host-range mutants of Caudoviricetes with different morphotypes infecting different genotypes of Escherichia coli from the ECOR collection, strong negative relationship was observed between replication rates and host-ranges (Keen, 2014). Also, in vitro experimental evolution of the Microviridae phage ϕX174 to Salmonella enterica was accompanied by a reduced ability to infect E.coli (Crill et al., 2000). Moreover, majority (but not all) of mutations present in the Cystoviridae ϕ6 phages that conferred an expanded host range imposed a significant cost for fitness on the original host, presumably due to antagonistic pleiotropy (Ferris et al., 2007; Duffy et al., 2006). More precisely, phenotypic and fitness assays showed that the proximate mechanism underlying host range expansion in P. syringae was an increase in the ability to attach to the novel host (Ferris et al., 2007). Also, Klebsiella phages with higher burst size phages were associated to a narrower host range compared to other phages with lower burst size phages that exhibited expanded host-range (Kęsik-Szeloch et al., 2013). As a conclusion, host-range mutations seem to induce a selective cost. However, little is known about the potential for subsequent compensatory mutations to ameliorate the initial costs of expanded host range mutations.

The aim of our study was thus to investigate the potentiality of selection of host-range mutant with restored fitness. We thus designed an experiment to (i) select a phage with expanded host-range and (ii) let natural selection to act and select adapted phages with increased fitness. Notably, our understanding of phage specialism and generalism depends on whether our view of bacterial diversity corresponds to phage's one. In other words, we might consider diversity where phages don't see any. In fact, phages may adapt to molecular pathways that

might be similar across phylogeny (because of molecular convergence due to environmental constraints applied to bacteria or horizontal transfers across species) which are completely different from the tools that scientists are using to describe bacterial phylogeny. More precisely, on the one hand, we will consider a bacteriophage as specialist if it infects only a few strains that are closely related based on their phylogenetical distances. Such distances can be based on different traits such as, among others, divergence among house-keeping genes (e.g. Multilocus sequence typing; (Maiden et al., 1998) or, at a larger genomic resolution, divergence among core- and pan-genomes (Zhou et al., 2020). Other classifications among bacteria have also been used (even today), such as presence of antigens presented at the surface of bacteria (serotypes) or presence of antibiotic resistance genes (Aminov & Mackie, 2007). As an example of bacterial diversity, the Salmonella genus has been classified with more than 2500 serotypes and approximately 4000 sequence-types (Alikhan et al., 2018). On the other hand, success or failure of bacterial infection by bacteriophages resides on the completeness of several steps: adsorption to bacterial cell surface-exposed molecules (or receptors), as well as injection, expression and replication of the viral genetic material within the host cytoplasm and finally the lysis of the cell to allow horizontal transmission. Bacteriophages are thus submitted to multiple mechanisms of resistances (reviewed in (Egido et al., 2022) acting concomitantly during infection of each host, bacteria being able to resist not only through variation of molecules involved at each step of the infection process (e.g. mutations on genes involved in LPS structure known as receptors; (Nobrega et al., 2018) but also thanks to accumulation of different types of antiviral mechanisms (virus nucleic acid degradation, Abortive infection, inhibition of DNA/RNA synthesis; (Tesson et al., 2022; Georjon & Bernheim, 2023).

Note that fitness is polysemic and can be evaluated in different ways. We choose to approximate phage fitness by registering bacterial growth inhibition in presence of phages with the following rational : increase in phage burst size and/or shorter latent period and/or higher adsorption rate (three parameters usually considered as participating to phage fitness (Abedon & Calendar, 2006) will lead to quicker infection of bacteria, inducing a decrease in bacterial growth until phage population overwhelm bacterial one until such a level that bacterial growth is no longer visible. Thus, by infecting bacterial population with different doses of phages (i.e. different multiplicities of infection), we considered that the minimum inhibition phage concentrations indicated phage efficiency to infect bacteria and decrease bacterial growth. In other words, the most efficient phage corresponded to the phage inhibiting bacterial growth at the lowest MOI. Because, we wanted to differentiate our fitness approximation to the ones present in literature, we used hereafter the term “virulence” as our fitness proxy.

The aim of our study was to understand the adaptive walk selected for a virulent bacteriophage (Tequintavirus) evolving in a complex environment composed of susceptible and resistant strains (from two different sequence types). From a single ancestor, five bacteriophage populations were evolved independantly in order to detect any potential convergence in phenotypes and/or genotypes accross replicates. It is important to note that only phage populations were able to evolve in this experiment: Salmonella cultures were kept evolutionarily naive by

bringing in fresh Salmonella cells after each coculture cycle. After realising serial passages of the bacteriophage population (i.e. Appelmans'protocol, (Burrowes et al., 2019), we observed a broader host-range and, more surprisingly, an increased virulence in the evolved compared to the ancestral bacteriophage population. Sequencing of all bacteriophage populations revealed multiple mutations appearing at the same loci (parallel mutations) in different genes. Notably, a lot of mutations were accumulating on the external side of several caudal proteins as represented on 3D reconstruction. Moreover, two parallel mutations showed to become fixed within the population before the other parallel mutations. These two mutations were present on the long tail fiber gene, a gene already known to influence bacteriophage host-range (Zhang et al., 2022; de Jonge et al., 2019). To directly evaluate the adaptive effect of these two parallel mutations, we introduced them into the ancestral genome by reverse genetics and showed that they participate in the increase in host-range but marginaly to the increase in virulence. Our study demonstrate that (i) experimental evolution in vitro of one bacteriophage allows selection in a short period of time of a generalist phenotype harboring a broader host-range as well as increased virulence and (ii) the first drivers of bacteriophages'evolution are proteins involved in recognition of bacterial receptors before intra-cellular mechanisms of resistance. From an applied perspective, our results pave the way on generating generalist therapeutic bacteriophages adapted to several bacterial targets prior any applications in order to decrease the probability of appearance of resistant bacteria that would invalidate treatments.

Materials and Methods

Bacterial and Bacteriophage Strains

Thirty-one isolates of *Salmonella enterica enterica* were sampled from swabs passed in a food processing factory in Poland, during a two-year period (2017-2019) and serotyped as Tennessee by Eurofins (Aix en Provence, France). These isolates were called hereafter by the prefix « SeeT » followed by a number from one to thirty-one (randomly chosen). Bacteria were systematicaly grown in LB (Lennox, Athena Enzyme Systems; Baltimore, MD, USA).

The bacteriophage used in this study was isolated from Marseille’s waste-water (M.AMP, November 27th 2017) stored in glass bottle. The waste water was first mixed (50µL) into a 96-well plate (Polypropylen) filled with 500µL of LB inoculated with 2µL of an overnight culture of SeeT2 with a 96-pin replicator (#140500, Boekel Scientific; Feasterville, PA, USA). Overnight co-culture was performed at 37°C within an incubator with ventilation (Aqua-lytic) and rotation at 450 rpm and 1.5mm orbital (Titramax 101 #544-11300-00; Heidolph Instruments, Schwabach, Germany). Next day, 50µL of Chloroform was added to the solution and left four hours

at 4°C. 2µL of the supernatant was then transferred in new 96-well plate made of polystyrene PS (#82.1581001; Sarstedt, Nümbrecht, Germany) filled with 200µL of LB supplemented in 10mM CaCl2 (Sigma-Aldrich, #C3881) inoculated with Boekel replicator with 2µL of overnight co-culture of SeeT2. Bacterial growth was then followed overnight within the spectrophotometer FLUOstar Omega (BMG Labtech, Ortenberg, Germany) at 37°C with 300 rpm orbital shaking. Based on the observation of a delay in bacterial growth, we then transfered the supernatant into a polypropylene tube (Eppendorf), add 50µL of chloroforme, centrifuge (10 min at 15,871 rcf, Eppendorf 5415 R) and mixed a dilution of the solution with top LB-agar (6g/L; #LF611001 Liofilchem, Italy) and 100 µL of overnight bacterial culture of SeeT2 in order to obtain isolated plaques. Five consecutive bottlenecks were then proceeded. Amplification of the bacteriophage was made in solid condition (double-layer method) and resuspended into SM buffer (NaCl 100mM, MgSO4-7H2O 10mM, Tris-HCl [pH=7.4] 50mM), centrifuged at 3,000 rcf for 10min (Eppendorf Centrifuge 5702R), the supernatant was filtered through 0.22µm Minisart polyethersulfone (PES; #16541--K; Sartorius, Göttingen, Germany) and stored at 4°C into 15mL tubes (#352096; Falcon, Corning, Mexico) before use. The isolated phage was called « Salten ».

Phage Morphology

15mL of a Salten solution (10^{11} PFU/mL) was distributed into 1.5mL polypropylene tubes and centrifuged for 1 hour at 16,000g at 4°C (Eppendorf Centrifuge 5415R). Pellets were resuspended in 100µL of 100 mM of ammonium acetate (NH4-CH3CO2, Sigma-Aldrich) and pooled into one tube to be once again centrifuged (16,000g, 4°C). Pellet was finally resuspended in 600µL of 100mM ammonium acetate and filtered through 0.22µm PES filter. Bacteriophages were adsorbed onto grid Formvar/carbon 300 (# CU 50/BX 9012.90.0000; Electron Microscopy Sciences, Hatfield, PA, USA) and contrasted with 2% uranyl acetate before observation through TEM electronic microscopy (JEM-1400Plus, JEOL, Akishima, Tokyo, Japan).

Experimental evolution

Eight out of the thirty-one SeeTs isolates were used in the experimental evolution: four that were sensible (SeeT2, SeeT4, SeeT7 and SeeT17) and four that were resistant (SeeT1, SeeT3, SeeT5 and SeeT6) to Salten. To prepare the stock solution of these 8 bacterial strains, we first inoculated 7mL of LB in 16mL Soda Glass Cell Culture Test tubes (#11823370; Fisher Scientific, Illkirch, France) from an isolated colony present on Petri dish and allowed overnight bacterial growth into a ventilated incubator (35°C with 150 rpm mixing; MaxQ 4000, Thermo Fisher). Next day, we filled each well of a 96 deepwell plate (1mL, Polypropylen; #135702; Dutscher, Bernolsheim, France) with 250µL of 60% (v/v) Glycerol (#G6279; BioXtra, ≥99% Sigma-Aldrich St. Louis, MO, USA) and eleven wells per strains (one strain per row, the twelfth column remaining empty) with 500µL of overnight culture. This « stock 96 deepwell plate » was then stored at -70°C (CryoCube F750h; Eppendorf).

Each month, one new deepwell plate was prepared with 500µL of LB inoculated by the eight bacterial strains according to the « stock 96 deepwells plate » with the help of the 96-pin Boekel replicator and let to grow overnight at 35°C - 450 rpm (Aqualytic ventilated incubator with Titramax 101, Heidolph). This latter plate (called hereafter « inoculation 96 deepwells plate ») contained approximately 10^{10} CFU/mL (estimation from easySpiral plater; #412 000, Interscience, Saint-Nom-la-Bretèche, France) and was then stored at 4°C and used when needed to inoculate new 96-well plates.

Salten was serial passaged at least seven times following the Appelman's protocol (Burrowes et al 2019). Briefly, one the one hand, each well of a new 96-well PS plate was first filled with 200µL of LB+CaCL2 (10mM) inoculated from the « inoculation 96 deepwells plate » with the help of the 96-pin Boekel replicator. On the other hand, phage solution was prepared as follow: each well of a 96-well polypropylene PP plate (#290-8353-03R; EVCORP, USA) was filled with 180µL of SM buffer in each well. 20µL of the undiluted Salten solution was then introduced into each well of the first column and, after mixing, 20µL was then transferred into the wells of the second column (i.e. 10% dilution) and so on until column 10 (that is approximatively a 10 log dilution from column 1 to 10), leaving the last two columns without phage solution. Finally, 2µL of each well of this PP plate were then transferred with the help of the 96-pin Boekel replicator into the PS plate. The eleventh column thus corresponded to positive control (i.e. bacterial isolate without phage) and the twelfth column to negative control (without bacteria nor phage). Bacterial temporal kinetic (37°C, 300 rpm double orbital shaking) was followed with the spectrophotometer FLUOstar Omega. After at least 16h of incubation, solution of each well presenting a delay in bacterial growth was harvested and mixed into a single 15mL Falcon tube. After adding 500µL CHCl3, mixing and centrifuging 10 min at 3,000 rcf and filtered through 0.22µm PES filter, the phage solution was stored at 4°C. Eventually, the phage solution served as a starting solution for the next passage following the same process as just presented. Phage concentration between each passage has not been estimated.

Estimation of host-range and virulence

Phenotype estimations of both ancestral and evolved phage populations were performed the same days in parallel. Prior any comparative experiment, we first estimated phage concentration by spot-assay method (Kropinski et al., 2009), that is spotting 10% dilutions of the phage population on a double-layer LB-agar containing 100µL of overnight culture of the most susceptible strain SeeT17. These phage titer estimations were made in order to adjust each titer and compare phenotypes based on similar multiplicities of infection between both ancestral and evolved phage populations.

We estimated host-range both in solid and liquid conditions. Concerning the liquid method, preparation of 96-well PS plates was similar as presented above (Experimental evolution) except for the preparation of the PP plate

containing phage dilutions. In fact, we only diluted phages on a range of 5 logs, column 1 to 5 being filled with dilutions of ancestral phage population and columns 6 to 10 filled with dilutions of evolved phage population. Bacterial growth was then followed overnight within the spectrophotometer FLUOstar Omega (BMG Labtech, Ortenberg, Germany) at 37°C with 300 rpm orbital shaking. Each comparison experiment was tested three times on different days.

Concerning the solid method, in order to normalize any potential effect of bacterial strain producing the tested phage population, we mixed each phage population (either ancestral or evolved) at a multiplicity of infection MOI ~0.001 with the most susceptible bacterial strain (SeeT17) using the double-layer method. Ten clear plaques (called « clones » hereafter) per population chosen according to distinct diameters were collected and transferred in 200µL SM buffer (+20µL CHCl3). After centrifugation, 3.5µL of the supernatant was dropped onto a bacterial lawn made of each of the eight bacterial strains and incubated overnight at 35°C (Memmert). Observation of presence/absence of plaques were recorded on next day, according to a visual evaluation (see exemples in Fig.S4). Each comparison experiment was tested three times on different days.

DNA Sequencing

Full genome sequencing of each of the eight bacterial strains used (SeeT1, 2, 3, 4, 5, 6, 7 and 17) were performed by the French National Reference Center for Escherichia coli, Shigella and Salmonella at the Pasteur Institute (Paris, France). Bacterial DNA was purified using the Maxwell 16-cell DNA purification kit (Promega) and sequenced by Illumina NovaSeq technology (paired-end). A Sanger sequencing of the cpn60 gene (Hill et al, 2006) was conducted on the 31 SeeTs isolates. Bacterial isolates were grown on LB-agar overnight at 35°C, and then one colony was picked up and added in 100µL of H2O in PCR tubes. After 10min of boiling at 95°C, 1.5µL was added in a PCR mix, following the recommandations of Meck supplier when using the Roche Taq DNA polymerase (5U/µL; #11146165001; Merck KGaA, Darmstadt, Germany) and supplemented in DMSO. The annealing temperature used for cpn60 primers (cp60 primers flanked by M13 universal primers, ordered at Eurofins Genomics France; Table S1) was set at 57°C and 35 cycles were necessary to amplify the cpn60 gene. Amplicons of 483bp were then sent for Sanger sequencing to Eurofins Genomics France (Nantes, France).

To extract DNA, phage populations were first grown on liquid condition within 96-well plate containing either the most susceptible strain SeeT17 infected by the ancestral phage or the eight strains infected by the evolved phages population. For each phage population, 15mL of lysate were centrifuged into several 1.5mL tubes (Eppendorf) at 15,871 rcf during 1 hour, and the pellet was resuspended into buffer A (10 mM Tris HCl, 2.5 mM MgCl2, 0.1 mM CaCl2, 100mM NaCl, pH 7.5) and pooled in one tube in order to again be concentrated (15,871 rcf during 1 hour). After resuspending the pellet into 100µL of Buffer A, genetical material (from bacterial origin) potentially surrounding phage capsids were eliminated by adding 10µL of DNAse I (1U/µL; #D5307;

Sigma-Aldrich), 5µL of RNAse A (10mg/mL; #EN0531; ThermoFisher) and 2µL of Dpn I (10U/µL; #ER1702; ThermoFisher) to the solution and incubating at 37°C. After 1h, 900µL of buffer B (10 mM Tris HCl, 2.5 mM MgCl2, 0.1 mM CaCl2, pH 7.5)) was added and tubes centrifuged during 1 hour (15,871 rcf). Pellet was resuspended into fresh buffer B and DNA was extracted using phenol-chloroform-isoamyl acid 25/24/1 (#77617; Sigma-Aldrich). After quantification with NanodropOne (Thermo-Fischer Scientific) and Qubit 4 Fluoremeter (Invitrogen, Thermo-Fisher Scientific, Waltham, MA, USA), we multiplexed the different DNA extractions using the NebNext Ultra II FS Library Prep Kit (#E7805, #E6440 and #E6177; NEB). Briefly, phages DNA was fragmented with a transposase enzyme and prepared for multiplexing according to the recommendations of the supplier for inputs over 100ng. Fragmented end-prepared DNA were ligated with Illumina adaptors and then sorted with beads to select fragment sizes between 150-250 bp, for a final size with primers between 270-370 bp. Adaptor-ligated DNA was enriched by 4 cycles of PCR. These amplicons were then cleaned and ligated with a unique pair of primers. Quality of the final library has been evaluated through Qubit 4 and fragments sizes were checked by migration using QIAxcel Advanced Instrument (QIAgen, Hilden, Germany). Fragments ready for sequencing sized between 280bp and 320bp. Prepared DNA has then been sequenced in paired-ends on our in-lab sequencer (iSeq100; Illumina).

To determine the order of arrival of mutations across serial passages, we designed primers flanking the mutations of interest in the genes coding for pb1, pb2 and the recombination related exonuclease (Table S1). Amplicons were obtained using the Q5 high-fidelity DNA polymerase (#M0491; New England Biolabs NEB) and sent for Sanger sequencing to Eurofins Genomics France (Nantes, France).

Bioinformatic analysis and Annotation

The eight SeeTs used in our experiment were genotyped using the core genome multilocus sequence typing (cgMLST) based on the analysis of 3002 genes in the soft core genome (Zhou et al, 2020 Genome research). PanExplorer online tool (Dereeper, 2022) was used for core-genome visualization and genetic diversity analysis between the eight SeeTs. DefenseFinder (Tesson et al, 2022) was used for the search of defense mechanisms against phages. Phaster (Arndt et al, 2016; Zhou et al, 2011) was used for the search of prophages in the eight SeeTs' genome. Dendrogram on all SeeTs was constructed using the nucleotide sequence of the cpn60 gene. The similarity matrix was obtained alining nucleotides in Muscle (Edgar, 2004) followed by a manual curation. Jmodeltest (Darriba et al. 2012) estimated that JC69 was the most suitable nucleotide substitution model, then it was run on PHYML (Guindon et al. 2009) with 1000 bootstraps.

After Illumina sequencing, phage reads quality has been controlled using FastQC 0.12.1 (Andrews, 2010). Primers were trimmed with Fastp 0.22.0 (Chen et al 2018). We followed the workflow recommended in Turner et al. (2021) for phage contigs preparation. The bacteriophage de novo genome assembly was carried out with

SPAdes 3.14.1 (Antipov et al 2002, Prjibelski er al 2020) with default parameters, resulting in a single contig of 110076 kb with high coverage and other very short contigs (less than 1200bp) with low coverage. To correct any assembly errors, the first contig of Salten and contigs of each evolved phages were polished with Pilon 1.24 (Walker et al 2014), using their respective reads. The new contig of 110 kbp has been annotated thanks to the the Bacterial and Viral Bioinformatics Resource Center (BV-BRC, https://www.bv-brc.org/) (Olson et al 2023), based on Tequintavirus annotation (Taxonomy ID = 187218) and structural genes were annotated manually based on Zivanovic et al (2014), Linares et al (2023) and using blastn or blastp on NCBI. Gggenes package (Wilkins D 2023) was used to generate the genome mapping of Salten. Breseq 0.38.1 (Barrick, 2014) was used as a pipeline for variant calling (Single Nucleotide Polymorphism or SNPs, deletions, insertions). The associated Gdtools COMPARE tool was used to visualize mutations present in each of the evolved phage populations and quantify their frequency (percentage of reads containing a mutation at a position of interest). Salten complete genome (including the two terminal repeated sequences) has been generated with PhageTerm tool (Garneau et al, 2017). Salten complete genome was deposited on EMBL-EBI with Accession Numbers …

Phage mutagenesis by Reverse-Genetics

In order to directly evaluate the phenotypic effect of two potential adaptive mutations (C to T at position 80453 and A to G at position 80495) identified within the gene coding for the Long Tail Fiber pb1 protein (79875bp-84026bp, positions gave by BV-BRC annotation on the 110kb genome of Salten) present in evolved phage populations (and absent from the ancestral one), we decided to introduced the two mutations by directed mutagenesis inside the gene coding for pb1 of Salten. To do so, we first confirmed the presence of mutations in the gene coding for pb1 in evolved phage populations by sequencing (Sanger; Eurofins, Nantes, France) the amplicon obtained from PCR using Q5 high-fidelity DNA polymerase (#M0491; New England Biolabs NEB) and the primers Salten-pb1-3183-F / Salten-pb1-4136-R primers (TableS1). After confirmation of the presence of the two potential adaptive mutations, we amplified by PCR the region surrounding the two mutations (Salten-pb1-3374-F and Salten-pb1-3557-Rv), using both evolved and ancestral Salten (negative control) DNA as matrix. PCR products were then introduced into pBBR1-MCS2 plasmid at XhoI and HindIII restriction sites (#R0146 and #R0104; New England Biolabs NEB). We then transformed (thermal shock) competent *E. coli* DH10β on LB-Agar supplemented with kanamycin (50µg/mL), Xgal (50µg/mL) and IPTG (10µM) with either plasmids. Transformation gave rise to clones harboring plasmid with an insert presenting pb1 partial sequence with or without the two potential adaptive mutations (called pBBR1-E or pBBR1-A, respectively). To control for any plasmid effect, we also transformed *E. coli* DH10β with the empty vector (called pBBR1-EV). White colonies were selected and PCR products (primers pBBR1-MSC2-F and Salten-3470-F; TableS1) were sequenced (Sanger, Eurofins, Nantes, France) to select appropriate bacterial clones. The three plasmids pBBR1-A, pBBR1-E and pBBR-EV were extracted using Monarch Plasmid Miniprep kit (#T1010; NEB) and following

supplier's instructions. Bacterial strain SeeT17 was then transformed with either pBBR1-A, pBBR1-E or pBBR1-EV by electroporation (~100ng/µL) using the MicroPulser electroporator (Bio-Rad, Hercules, CA, USA) on Ecoli1 program and then plated on LB-Agar supplemented in kanamycin (50µg/mL). Resistant colonies were selected and colony-PCR amplicons (primers pBBR1-MSC2-F and Salten-pb1-3470-F; TableS1) were sent for sequencing. Transformed SeeT17 with correct inserts were grown in LB supplemented with kanamycin (50µg/mL) and, at an optical density OD=0.2, we added the ancestral phage Salten (MOI = 0.001) in order to allow natural recombination between the phage and the insert present on plasmid. After an overnight co-culture, phages were recovered after centrifugation (30 min at 3,000 rcf) and filtration of the supernatant (0.22µm; PES #16541-K, Sartorius). Phages coming from co-culture with SeeT17 transformed with pBBR1-E, pBBR1-A or pBBR1-EV were respectively named rE_Salten, rA_Salten and rEV_Salten.

In order to reveal the phenotype due to the presence or absence of the two potential adaptive mutations, we mixed following the double-layer method either filtrate (rE_Salten, rA_Salten or rEV_Salten) with one of the four strains resistant to the ancestral phage Salten (SeeT1, SeeT3, SeeT5, SeeT6) as well as one susceptible strain (SeeT17). In cases of apparition of plaques, isolated plaques were picked and resuspended into 200µL of SM buffer (+20µL chloroform). One microliter was used as DNA matrix to produce PCR amplicons with the Phusion High Fidelity Taq Polymerase (#M0530; NEB) and new primers (Salten-pb1-3183-F and Salten-pb1-4136-R; TableS2). In order to to avoid any amplification of plasmids, note that these latter primers are targetting a pb1 phage region outside the sequence inserted into the pBBR1 plasmid. Moreover, to confirm that the phenotype was not due to a contamination made by evolved phage, we also performed PCR (and Sanger sequenced) on the isolated plaques with primers targeting a region harboring a specific signature of either the ancestral or evolved bacteriophage (primers Salten-pb2-8720-F and Salten-pb2-9129-R; TableS2).

The virulence of rE_Salten was evaluated in 96-well PS plates (liquid method), using the same preparation as above (experimental evolution, estimation of host-ange and virulence) except for the preparation of the PP plate containing phage dilutions. In fact, we diluted rA_Salten phages (corresponding to the ancestral population) on a range of 5 logs, column 1 to 5 and columns 6 to 10 were filled with dilutions of rE_Salten phages. Bacterial growth was then followed overnight within the spectrophotometer FLUOstar Omega (BMG Labtech, Ortenberg, Germany) at 37°C with 300 rpm orbital shaking. Each comparison experiment was tested three times on different days.

Statistical analysis

Data were analyzed using R software, version 4.3.0 (2023-04-21, R Core Team) implemented in Rstudio version 1.2.5042 (2020-04-01, RStudio team, 2020). We estimated phage's impact on bacterial growth in liquid cultures

using bacterial kinetic data of optical densities (Fig. S2). For each MOI, a Virulence index (Vi) was obtained following the formula (Storms et al 2020):

$$Vi = 1 - (AUC / AUCc)$$

where AUC corresponds to the area under the curve of bacterial growth in presence of phages and AUCc the area under the curve of bacterial growth control (i.e. without phage). We computed the AUC with the linear option of the MESS package (Ekstrom 2022). Concerning the phages' phenotypic characterization experiments, we analyzed the Vi data (MOI=0.01) using a linear mixed-effect model with identity of phages (n=5), identity of bacterial strains (n=8) nested into ST (n = 2) and their interaction as main effects, and the experimental plates (n=15) as random factor. Concerning the reverse-genetics experiment, we analyzed the Vi data (MOI=1 and MOI=0.01) using a linear mixed-effect model with identity of phage (n=2), identity of bacterial isolates (n=8) nested into ST (n=2) and their interaction as main effects, and the replicate (n=3) as random factor.

Analysis of spot profiles on double-layer solid cultures, which are qualitative data with three ordinal possible outcomes, were not fitting an ordinal logistic regression due to one outcome being largely represented compared to the two others among evolved phages. We therefore attributed a score to each outcome in order to generate quantitative data: « Resistant » = 0, « Turbid » = 5 and « Clear » = 10 for each individual bacteria-phage interaction (n=10). We then cumulated the ten scores for each given phage infecting a given bacterial lawn and we analyzed the cumulated scores using a linear mixed-effect model with identity of phages (n=4), identity of bacterial lawn (n=8), and interaction as main effects. We used replicate as random effect.

Statistical models were followed by type III ANOVA (package car, Fox J, Weisberg S. 2019) and posthoc contrasts on marginal means with the Tukey method (package emmeans, Lenth RV, 2020) and, when needed, one-sample t tests against 0 with correction for multiple testing (Benjamini & Hochberg correction). Ggplot2 package (Wickham H, 2009) was used to design plots. All R scripts and datasets used are available on GitLab at https://src.koda.cnrs.fr/MAURINAmandine/Salten

Results

Bacterial strains characterization

Over a two-year period, 31 isolates of *Salmonella enterica enterica* serotype Tennessee (SeeT) were sampled in a food processing factory. Among them, eight strains were randomly picked to be studied in more detail. O:H serotyping revealed that they belonged to O:6,7:z29 and cgMLST genotyping clustered them within two Sequence Types (STs): ST319 (SeeT1, SeeT3, SeeT5 and SeeT6) and ST5018 (SeeT2, SeeT4, SeeT7 and

SeeT17). Genomes are available on Enterobase through barcodes SAL-QB8957AA to SAL-QB8964AA. Core-genes represent 90.7 % of the genomes, with additional 8.6% of dispensable genes and 0.7 % of strain-specific genes. Clustering based on presence/absence of genes in the accessory-genome (PanExplorer, Dereeper, 2022) confirmed the separation in two STs (Fig.1A) with 300 to 354 different genes between the strains from different STs (Fig.1B). Interestingly, some of these different genes were involved in defense mechanisms. In fact, after scanning all eight genomes with DefenseFinder software (Tesson et al. 2022 Nat Comm) we detected that strains allocated to ST319 harbored two anti-phage mechanisms (CRISPR cas class 1 subtype I E system and Septu) which are not found in ST5018, and strains allocated to ST5018 harbored the Mokosh type I C defense mechanism. Despite the overall polymorphism among strains, the ones belonging to ST5018 harbored more similarities to each other (22 to 38 different genes) than strains belonging to ST319 (19 to 100 different genes). Moreover, when looking more carefully at genes coding for potential phages receptors such as genes implicated in the lipopolysaccharide synthesis, we detected amino-acid differences between STs on two genes (waaK and wzxC) involved in the O-antigen synthesis (Fig.S1AB). We further looked for differences between STs on FhuA, another potential phage receptor, and found that the two STs differed on two amino-acids located in the inner-part of the bacterial membrane, indicating that these two amino-acids should not have any interaction with the phage (Fig.S1C).

Prophages were detected by Phaster in the eight SeeTs used for the experimental evolution. All strains have 3 intact prophages and between 4 to 7 incomplete or questionable prophages, most of them belonging to Enterobacteriacea phages (Salmonella phages, Escherichia phages, Entero phages, see Table S2). The bacterial lawn of some SeeTs on LB agar sometimes showed turbid plaques without adding phages, as was often the case for SeeT2, 3 and 5.

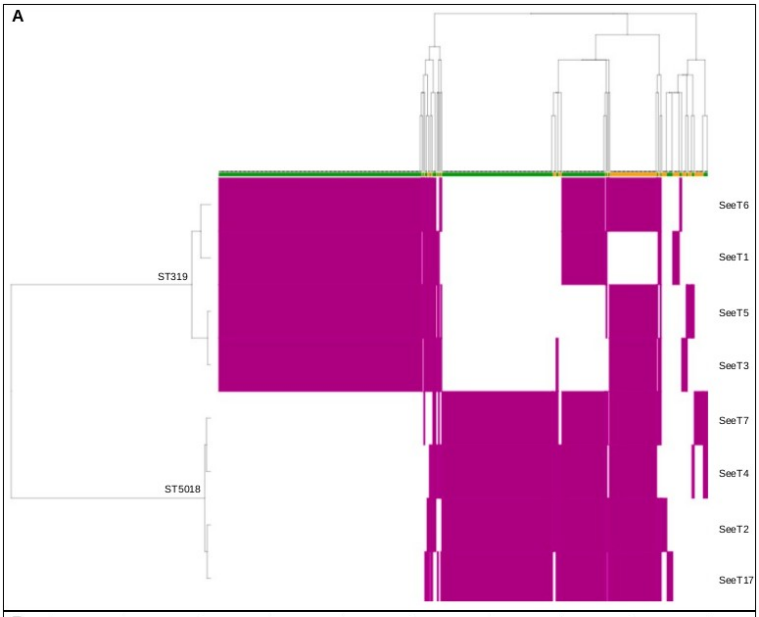

B

	SeeT17	SeeT2	SeeT4	SeeT7	SeeT1	SeeT3	SeeT5	SeeT6
SeeT17	0							
SeeT2	22	0						
SeeT4	30	24	0					
SeeT7	38	28	26	0				
SeeT1	346	348	350	354	0			
SeeT3	341	345	343	351	99	0		
SeeT5	344	348	344	354	100	19	0	
SeeT6	300	300	310	310	60	55	54	0

Figure 1. Genetic diversity in the accessory-genome of the eight SeeTs used for the evolutionary training. A- Presence/absence (respectively purple/white) genes clustering heat-map generated by PanExplorer on the accessory-genome. The dendrogram (on the top) shows hierarchical genes clustering (colored green and yellow alternately). The dendrogram derivated from the heat-map (on the left) illustrates the genetic relationship among the SeeTs. **B-** Matrix used to generate Fig.1A, listing the number of different genes in the accessory-genome, between SeeTs. SeeT17 genome was used as referent strain. SeeTs are ordered according to their ST.

Bacteriophage characterization

Transmission electron microscopy (TEM) revealed a T5-like Siphophage morphology, with a long non-contractile flexible tail of about 180 nm, attached to an icosahedral head of 60 nm of diameter (Fig.2A).

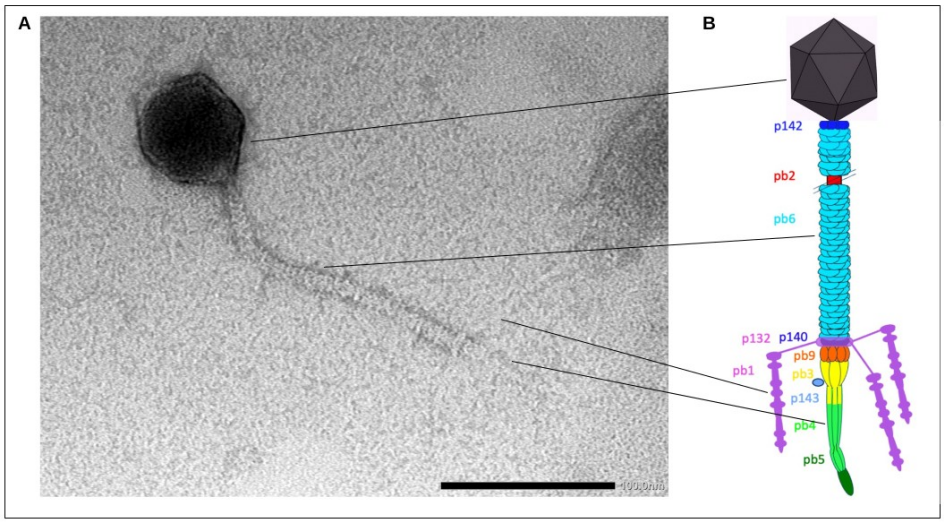

Figure 2. Morphology of the *Tequintavirus* Salten A- Transmission electron microscopy (TEM) **B-** Schematic structure of T5 adapted from Zivanovic et al. 2014. Tail Tube Protein pb6 (TTP_{pb6}, light blue), L-shaped tail fibers pb1 (LTF_{pb1}) and their attachment ring p132 (purple), and the distal tail proteins pb3, and pb4 (yellow and green, respectively). The scale bar represents 100 nm.

The isolated phage harbors a genome of 118 385 base pairs (sequencing mean coverage ~162x) with a ~39% GC content. The closest described phage is the *Escherichia* phage HildyBeyeler strain Bas33 (86% of blastn identity, GenBank accession: MZ501074.1). It was called « Salten » and thus represents a new phage from a new species within the *Tequintavirus* genus. The structure of T5 tail being available (Linares et al, 2023), we could describe the structural codal part of Salten (Fig.2B). T5 tail is composed of a tail tube formed by the stack of forty trimers of the Tail Tube Protein pb6 (TTP_{pb6}, cyan, visible on Fig.2A). TTP_{pb6} is composed of two tail tube domains (TTDs) and an Ig-like domains. The forty first ring towards the distal extremity of the tail is made by a trimer of p140 (dark blue), formed of two TTDs, which is buried under the collar. A dodecamer of p132 (purple), an Ig-like fold, forms the collar, which serves as an anchor for the three lateral Long Tail Fibers formed by pb1 (LTF_{pb1}, purple, visible on Fig.2A). Below p140, the tube extends by the Distal Tail Protein (DTP_{pb9}, orange), formed by a TTD and an oligosaccharide binding folds (OB-fold) domain. The tube is closed by the Baseplate Hub Protein pb3 (BHP_{pb3}, yellow), which C-terminus starts the central fiber that is continued by pb4 (light green, visible on Fig.2A), as a trimer of five FNIII domains and a spike, also decorated with small domain. At the extremity of the central fiber is located the Receptor Binding Protein pb5 (RBP_{pb5}, dark green). The length of the tube is determined by the Tape Measure Protein pb2 (TMP_{pb2}, red), which is located in the lumen of the tail as a long coiled-coil, its C-terminus interacting with BHP_{pb3}.

Salten's host-range was tested against the eight bacterial strains of SeeTs both under liquid (96-well plate, Fig.S2) and solid (double-layer assay) conditions. Under liquid conditions (black crosses in Fig.3A), we calculated the virulence index (Vi) to quantitatively evaluate the ability of Salten to infect each bacterial strain. Note that Vi∼0 indicates that bacterial growth was not affected by the presence of phage while Vi∼1 indicates an inhibition of bacterial growth in presence of phage. We first checked for any effect of the day (one 96-well plate per day was prepared) on virulence indexes and no effect was observed ($Chisq_{14}$ = 11.213, p = 0.669; type II ANOVA). The phage was overall more virulent on ST5018 compared to ST319 (linear mixed model, $Chisq_6$ = 119.075, p < 0.001, ST319 emmean = 0.121 [0.0826 - 0.158] and ST5018 emmean = 0.609 [0.5708 - 0.647]). Inside each ST, phages had the same impact on virulence as no difference were observed on virulence indexes (p <0.001; posthoc comparison on marginal means by pairs between bacteria and by ST). SeeT6 (ST319) and SeeT7 (ST5018) were two exceptions. Indeed the ancestral phage Salten was more virulent on SeeT6 (values of virulence index not different from 0 ,t_{112} = 0.010, p = 0.992, post-hoc comparison using Kenward & Roger method with Benjamini & Hochberg correction),which implied virulence indexes differences compared to SeeT1 (t_{98} = 3.459, p = 0.036) and SeeT5 (t_{98} = 3.468, p = 0.035). Concerning SeeT7, it was alternatively and unpredictably sensitive or completely resistant, whatever the experiments done in liquid or in solid cultures. We then observed significant differences with SeeTs from the same ST (SeeT2: t_{98} = 8.379, p < 0.001; SeeT4: t_{98} = 7.713, p < 0.001; SeeT17: t_{98} = 8.655, p < 0.001).

Concerning the host-range characterization in solid conditions (Fig.3B), ten clones of Salten (i.e. ten isolated clear plaques obtained on SeeT17 bacterial lawn) were spotted on bacterial lawn of each of the eight bacterial isolates. Plaques were visually assigned to « clear » or « turbid » or « no plaque » profiles (see exemples in Fig.S3). Globally, 64.2% of spots showed clear plaques, 28% were turbid, and we were not able to observe any plaques in 7.8% of the spots. Phage spots on SeeT1 produced a majority of turbid plaques and very few clear plaque. SeeT3, 5 and 6 showed all spot profiles (clear, turbid and no-plaque). SeeT5 and SeeT6 had a majority of no-plaque. Salten's clones on SeeT7 presented for unidentified reasons high heterogeneous profils (clear or no-plaque) depending on the replication days without showing turbid plaques. SeeT2, 4 and 17 were highly sensitive to Salten's clones since all the spots were clear. Statistical analysis on cumulated scores showed different virulence of Salten according to the ST (linear mixed model with bacteria nested in ST followed by a type III ANOVA; Chisq1 = 8.078, p = 0.004) with a lower virulence attributed to ST319 (emmean = 57.1 [33.1 - 81]) compared to ST5018 (emmean = 91.7 [67.7 - 116]; post-hoc contrast averaged over the levels of bacteria, t_{14} = -4.368, p = 0.001).

Phenotypic characterization of evolved phages populations

Phage host-range expansion depends on the ability of phages to reproduce and generate adaptive mutations. We first tried to evolve Salten under liquid conditions but we were unable to recover any viable phage when Salten was inoculated into any of the resistant bacterial genotype cultures belonging to ST319 (data not shown).

Following the Appelman's protocol (Appelman, 1931; Burrowes et al 2019), we experimentally evolved Salten in liquid conditions by mixing translucent solutions resulting from inoculations of Salten and the eight non co-evolving bacterial strains (one bacterial genotype per well of the 96-well plate), knowing that four of them were susceptible (strains from ST5018) and four resistant (strains from ST319) to Salten (called hereafter « ancestral phage population »). We realized such experimental evolution five times (five « lineages ») independently. The first lineage was produced by realizing six serial passages of the phage population (called « SaltenE1 »). Host-range and virulence index of both the ancestral (Salten) and evolved (SaltenE1) populations were then compared in the same conditions and we observed that the evolved phage population presented an expanded host-range and increased virulence. Several months later, we realized seven serial passages for three additional independent lineages (SaltenE2, SaltenE3 and SaltenE4) and we could observe results similar to SaltenE1. The genomics and bioinformatics analysis on SaltenE1 to SaltenE4 (see below) were then performed. Finally, when we were sure that no Salten phages had been used in the laboratory for 18 months, we realized a new experimental evolution (SaltenE5; 8 passages) that, again, presented similar results than lineages SaltenE1, E2, E3 and E4 (Fig. 3A) showing that previous phenotypes were not due to accidental contaminations.

In order to avoid any seasonal effect on our results, we compared at the same period the bacterial growth of the eight strains in presence of either one evolved phage population versus the ancestral one. We first tested for any potential effect of running the experimental replicates over several days (one 96-well plate per day) and found no significant effect (linear mixed-effect model with plate as main effect, bacterial identity and phage identity as random factors, $Chisq_{14} = 5.175$, $p = 0.983$). Evolved phages had a higher virulence (emmean = 0.888 [0.863 - 0.913]) overall compared to their ancestor (emmean = 0.365 [0.339 - 0.390]) (Fig. 3A and S3; linear mixed-effect model, effect of evolutionary status Chisq1 = 150.202, $p < 0.001$; posthoc contrast averaged over bacterial strains, $t_{210} = -30.628$, $p < 0.001$). Each evolved phage populations SaltenEs had the same virulence on each bacterial strains. Indeed no significant difference among virulence indexes of SaltenE populations between ST was observed ($t_{70} = -0.450$, $p = 0.6544$; posthoc comparison over the levels of phages and bacteria, following a type III ANOVA on a dataset keeping only virulence indexes of SaltenE populations and a linear mixed-effect model in which bacterial strains were nested in ST). Moreover, virulences of SaltenEs populations were comparable between bacterial strains inside each ST (p between 0.778 and 1.000, posthoc comparison of phage by ST over some or all levels of bacteria).

Evolutionary theory predicts that the presence of novel potential hosts will apply selective pressures on a phage population that could drive two outcomes. First, the phage population could evolve a generalist phenotype with the capacity to target multiple hosts. Alternatively, the phage population could diversify into multiple subpopulations each specialized to a different host. To distinguish between these possibilities, we obtained phage lysates from the evolved

Since previous data were obtained in liquid conditions, the observed phenotypes were due to a populational effect. In order to evaluate the within-population variance of the phenotypes, we evaluated the frequency of phage clones isolated from each population. We thus collected on a SeeT17 bacterial lawn (this strain being the most susceptible one) ten isolated lysis plaques per evolved phage population (from SaltenE1, SalteE2, SaltenE3 and SaltenE4) and realized a spot assay on each bacterial isolate. Interestingly, 89% to 100% of the spots were clear on the eight bacterial isolates tested (Fig.3B). Interestingly, 6.4% and 4.2% of phages isolated from SaltenE1 harbored respectively no-plaque and turbid profiles and SaltenE4 generated 0.4% of no-plaque and 0.4% of turbid plaques.

Analysis of spot profiles were not fitting an ordinal logistic regression. We therefore attributed a score to each profile in order to generate quantitative data (see Material & methods for more details). We observed a significant higher number of clear plaques when bacterial lawn were in contact with SaltenEs clones. Indeed the evolutionary status (ancestral or evolved) had a significant effect on scores ($Chisq_1 = 43.195$, $p = 4.955e-11$; type III ANOVA), with a significant difference between ancestral and evolved phage populations (post-hoc contrast by pair between the evolution statue; $t_{102} = -10.015$, $p < 0.001$). Regarding only the evolved phages populations, no difference of plaques profiles between ST was observed ($t_{62} = -0.370$, $p = 0.712$; Type III ANOVA following a linear mixed model based on phages and bacteria nested in ST). Also, no difference between SaltenE2, E3 and E4 were observed (posthoc contrast averaged over the levels of bacteria done after a full model of interactions and a type III ANOVA; p between 0.230 and 0.985). However SaltenE1 had significant different virulent indexes compared to the other SaltenEs ($p <0.001$). Indeed SaltenE1 was the only phage population to generate turbid plaques or no-plaque on all bacteria lawn.

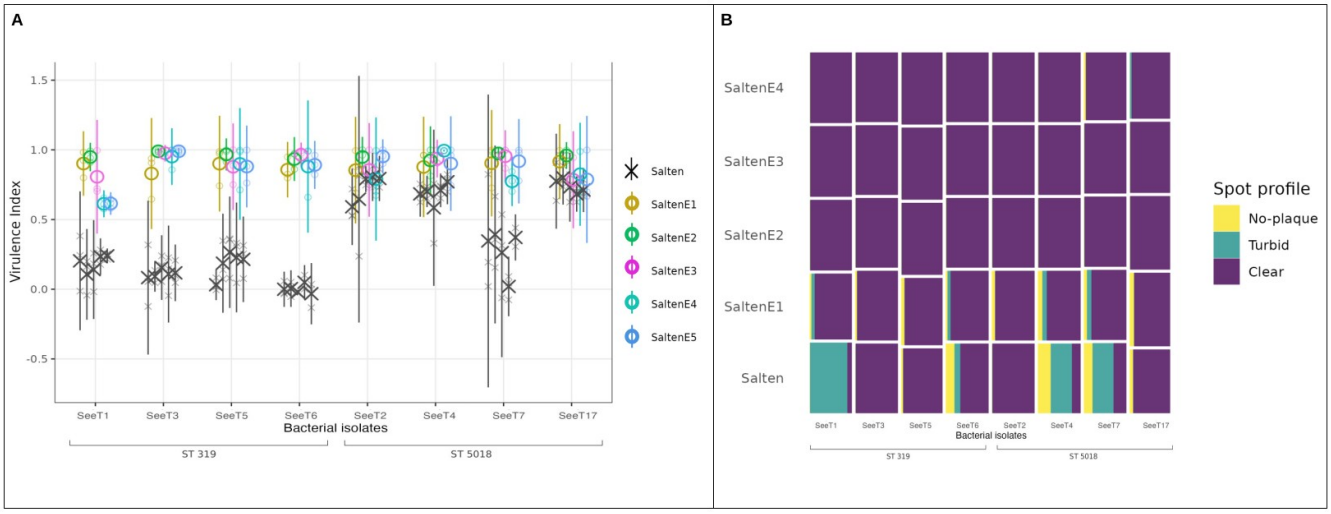

Figure 3. Phenotypic characterization (host-range and virulence) of the ancestral (Salten) and the evolved (SaltenE) phage populations on the eight *Salmonella enterica* serotype Tennessee (SeeT) genotypes according to their sequence type (ST319 or ST5018). **(A)** Evaluation in liquid condition of the phage virulence index at MOI=0.01, in presence of ancestral (black cross) or experimentally evolved (colored circles) phage populations (**B)** In solid condition, proportion of phage lysis plaque profile (clear, turbid, no-plaque) obtained after spoting of ancestral (Salten) or experimentally evolved (SaltenE1 to E4) phage populations. These experiments were conducted in biological triplicate.

Profiles of infection of the ancestral (Salten) and the five evolved (SaltenE) phage populations have also been tested in solid condition (spot assay) against other eighteen isolates of *Salmonella enterica* that we had in stock in addition to the eight SeeTs strains used for the experimental evolution (Fig.4). Salten provoked clear spots on 11/26 isolates, turbid spots on 10/26 and one bacterial strain SeeT18 was resistant (no plaque observed) in addition to SeeT3, 5, 6 belonging to ST319. SeeT7 was still an exception, with no plaque were observed. In contrast, the five SaltenE populations were able to infect the eighteen other bacterial isolates (clear or turbid plaques) except SeeT18. According to these results, we Sanger sequenced the cpn60 gene of all strains (Hill et al 2004 Genome Res) and found out that all bacterial strains on which turbid profiles were observed corresponded to the same cluster as SeeT1, SeeT3, SeeT5 and SeeT6 that is belonging to the ST319 (Fig.S5). Interestingly, strains on which clear profiles were observed corresponded to the same cluster as SeeT2, SeeT4, SeeT7 and SeeT17 that is belonging to the ST5018 except SeeT14 and SeeT21 that clustered within ST319 strains. Moreover, based on cpn60 sequencing, the strain SeeT18 clustered outside the two other groups. We thus re-sequenced this strain and it turned out to belong to another serotype (Mbandaka). Unfortunately, we could not characterized by cpn60 five strains (SeeT9, 15, 19, 25 and 27), so we did not showed their results on Figure 4. As a partial conclusion, experimental evolution on eight strains belonging to two sequence types allowed host range extension on other strains belonging to the same sequence types as well as another serotype (SeeT18).

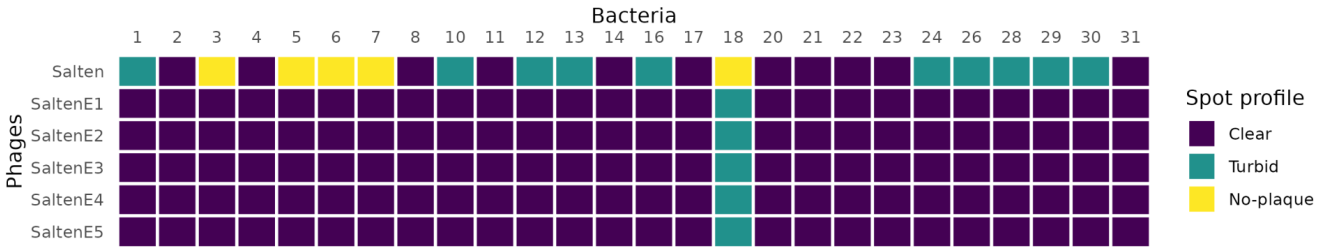

Figure 4. Spots profiles induced by ancestral (Salten) and evolved (SaltenE) phage populations on thirty-one bacterial isolates of *Salmonella enterica*. The spotting assay was conducted three times independently.

Genetic diversity and impact on proteins

To better understand molecular mechanisms underlying adaptation leading to host-range expansion and increased virulence, we sequenced the whole phage DNA of both ancestral (Salten) and evolved (SaltenE1, E2, E3 and E4) populations. Firstly, we checked that the phenotype observed in the evolved phages populations corresponded to a genotype similar to the ancestral genome in order to eliminate any contamination hypothesis that could have lead to this phenotype. After alignments of the evolved reads against the genome of Salten, around 90% of the evolved reads mapped against the ancestral genome Salten. Secondly, we indexed mutations, following a variant calling using breseq tool that highlighted mutations present within the four SaltenE populations (Fig. 5A). Overall, 2% of positions corresponded to indels and 98% to SNPs, with a hot spot of mutations detected within genes before and inside the coding structural part, from 75kb to 100kb. Interestingly, SaltenE2 and SaltenE4 had common mutations with a frequency of more than 50% in the phage-associated recombinase, while mutations shared by three to four SaltenE populations (called hereafter « parallel mutations ») were identified in structural and non-structural genes. Notably, parallel mutations were detected in genes coding for DNA modification or replication enzymes such as endonuclease, phage related recombinaison exonuclease, and Deoxyuridine 5'-triphosphate nucleotidohydrolase (dUTPase). More over, several parallel mutations accumulated in the genes coding for proteins involved in caudal structure known to participate to the host-range. We present below, gene by gene and protein by protein the observed polymorphisms according to the tail structure presented in Fig. 2B.

SNPs frequency and their detection in each evolved phage populations are represented in Figure5A. Thanks to knowledges on the codal structure, it was possible to localise the mutations with dissimilar properties or weakly similar properties (conservative mutations having no or little impact on the change of specificity of substrate binding) on the structure of the proteins (Fig.6ABCDEF). The gene coding for TTP_{pb6} (1392bp) harbored 119 SNPs shared between three evolved populations on which 18% were non-synonymous (Fig.5A). The mutation rate in the tube domain was at 3.3%, whereas it goes up to 20,7% in the Ig-like domain. Mutations in this domain were mainly located in the variable loops, known to be responsible for ligand binding (Fig.6CD). The gene coding for pb4 (2103bp), which is the penultimate protein before the irreversible receptor-binding protein pb5,

harbored 92 parallel SNPs shared by the four evolved populations on which 15% were non-synonymous. Within-population frequency of almost all of these SNPs were above 50% within SaltenE1 and SaltenE2 and between 25% and 75% within SaltenE3 and SaltenE4. Moreover, 13 SNPs (on which 54% were non-synonymous) were common to SaltenE1, E3 and E4. The gene coding for pb3 (2850bp) harbored 107 parallel SNPs shared by the four evolved populations on which 21% were non-synonymous. Twenty-one SNPs were common to three SaltenEs: 16 shared by SaltenE1, E3 and E4 (9 were non-synonymous), 3 shared by SaltenE1, E2 and E4 (all synonymous) and 2 shared by SaltenE2, E3 and E4 (one non-synonymous). Non-synonymous mutations in pb4 and the BHP_{pb3} (Fig.6CD) were concentrated in the FNIII domains and in the decorative domains of the spike, domains that are also proposed to increase infectivity by binding polysaccharides. Concerning the gene coding for pb9 (615bp), the coverage was too low to conclude on any mutations accumulation (less than 10x). Genes coding for p138 (369bp) and p139 (405bp) presented respectively 20 and 27 parallel SNPs on which only one in p138 and one in p139 were non-synonymous. The p140 coding gene (897bp) had 38 parallel SNPs on which 42% were non-synonymous. p140 being the Baseplate Tube Protein completely surrounded by the collar which does not have contacts with the cell surface, the mutation rate bared only at 1.3% at relatively low frequencies, coherent with the fact that it does not interact with the host surface. The gene coding for p132 (423bp) harbored 11 parallel SNPs shared by the four evolved populations on which 36% were non-synonymous. SaltenE1 ad E2 had these mutations at a frequency of more than 50%, whereas the frequency was under 50% for SaltenE3 and E4. The collar protein Ig-like p132 connecting pb1 protein to p140 had a mutation rate at 12.1% and as for TTP_{pb6}, mutations were mainly located in loops (Fig.6CD). Following the visualization of non-synonymous mutations on tail proteins in the evolved phages and knowing that some tail structural proteins are decorated with accessory domains or are composed of structural domains that either have protein or oligosaccharide binding folds, it is interesting to note that mutations were mainly located i) on the surface of the proteins and ii) in the decorations domains (Fig.6BCDE).

The case of the gene coding for pb2 (3708bp) is interesting because it is the gene that harbored the most parallel SNPs since more than 5% of the gene length was concerned by mutations. More precisely, 101 and 89 SNPs were present in four and three evolved populations respectively on which 11% and 29% were non-synonymous, respectively. Impact of non-synonymous mutations is more complicated to analyse. First, the structure of TMP_{pb2}, except for the 35 C-terminal, is not known. Second, residues 420 to 891 (i.e. 471 residues) of the ancestral phage TMP_{pb2} did not align at all to T5 TMP_{pb2}. This region corresponded to that of higher variability when comparing TMP_{pb2} sequences from the databases. The two proteins however only had 16 residues difference in length. In the C-terminus of TMP_{pb2}, bares a hydrophobic region, proposed to insert in the outer-membrane to form the DNA channel. It also bears a carboxypeptidase motif (Boulanger et al, 2008, Linares et al, 2023). Neither of these motives were affected by evolved mutations, and the ancestral sequence matched that of T5. Intrigued by this high number of parallel SNPs, we looked at their order of appearance through a PCR amplification and Sanger sequencing at passages 1, 3 and 5 of the experimental evolution. The majority of SNPs

appeared between the passage 4 and 5 in SaltenE1 and SaltenE2, and passage 6 and 7 in SaltenE3 and SaltenE4, even if we observed small differences in mutational profiles according to each evolved population. For exemple, one SNP appeared between the passage 4 and 5 within SaltenE3 population whereas some secondary peaks were observed as well in SaltenE1, E2 and E4, showing a transient co-existence of alleles over time.

Looking deeper for the mechanisms of « one go » acquisitions of these multiple parallel mutations, we analyzed more carefully the Salten's ancestral population sequencing data and considered the small contigs (< 1,200bp) that were first removed from the analysis because of their very low coverage (<0.5%) and high genetic diversity. We then aligned these small contigs present in the ancestral population with the highly mutated regions present in evolved populations. Interestingly, for 2 different region of pb2 gene (553bp - 1116bp and 1794bp - 2026bp; blue rectangles in Fig.5B), we found a >99% versus 85% similarity with evolved and ancestral phage population consensus sequence. In order to understand if these regions could be considered as « hypervariable », we aligned 100 sequences of pb2 proteins registered on NCBI as well as our ancestral and evolved sequences and we detected high variability in these same regions (Fig.5B, red rectangles).

Other caudal genes are also concerned by these higher percentage of similarities of the sequence of evolved phage population with the secondary genomes present in ancestral phage population. When they were blasted against the consensus evolved gene coding for p132, 100% of similarities was found *versus* only 73% when blasted against the ancestral gene. For pb3, we found 3 regions (1-854bp, 1272-1746bp and 2253 - 2701bp) with similarities above 99% for the evolved gene *versus* 76% for the ancestral gene. For pb6 gene, two small contigs (462 - 761bp and 1277 - 1407bp) harbored >98% *versus* 81% and 76% similarities of evolved and ancestral genes, respectively. For pb4, the region 205 - 957bp presented >99% *versus* 74% similarities of evolved and ancestral genes, respectively. As a partial conclusion, these analyses suggested that some phage regions are hypervariable and present in populations purified after several bottlenecks and that some these sequences can be adaptive and selected during evolution.

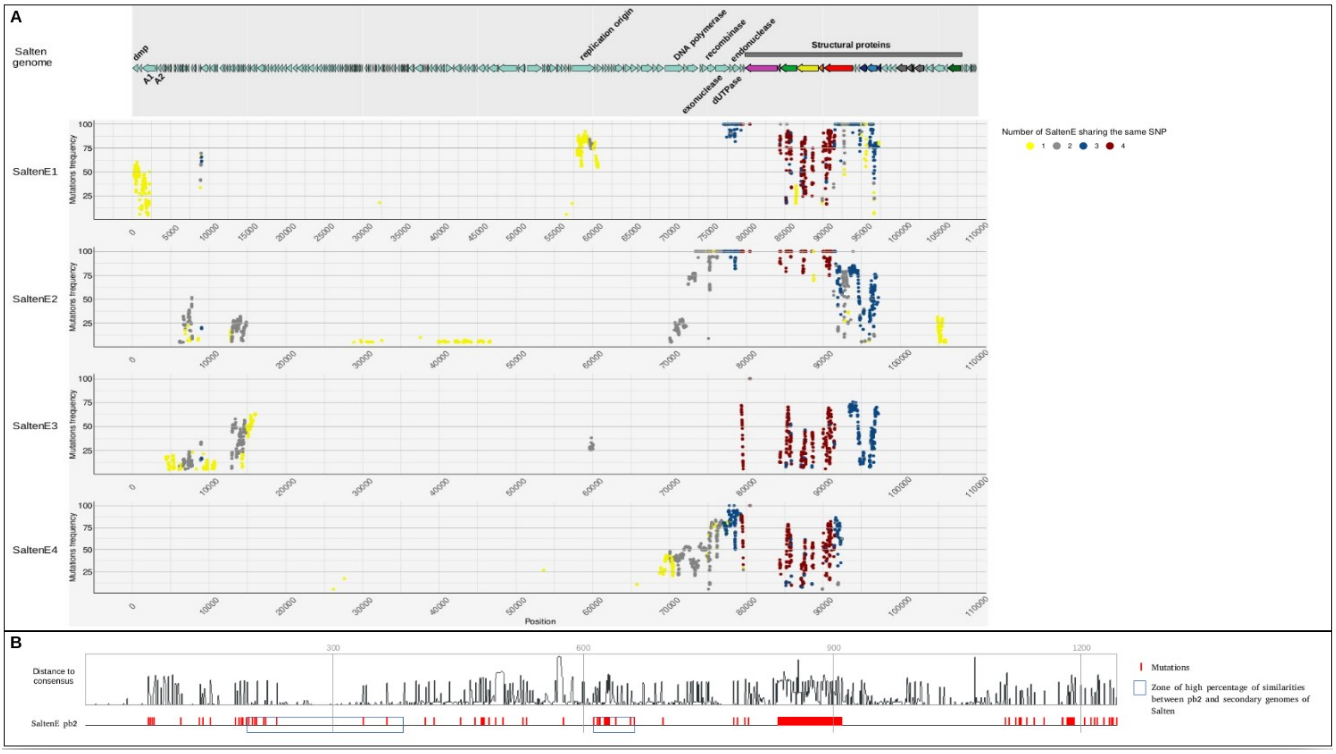

Figure 5. Frequency of mutations present in four independant experimentaly evolved (SaltenE) phage populations according to the ancestral (Salten) genome map. A- Visualization of mutations across full Salten genome. Colors of each mutation correspond to its degree of convergence over populations : yellow mutations are present in only one evolved population, gray in two, blue in three and red in four evolved (SaltenE) populations. **B- Detail of pb2 protein polymorphism.** First graph represents distance to consensus over 100 pb2 sequences downloaded from NCBI. Second graph with red flags represents positions at which we observed mutations into three or four evolved populations. Blue rectangles represent pb2 regions with low sequencing coverage within the ancestral (Salten) phage population.

Particular case of pb1 genetic diversity

The last caudal protein to be considered was the gene coding for pb1 (4152bp) that harbored only two SNPs (transition C to T at position 80453 and transition A to G at position 80495) present within the four evolved (SaltenE) phage populations. These two SNPs were present in 100% of the reads of SaltenE3 and E4 (~120X to ~200X of coverage) as well as SaltenE1 and E2 even though the coverage was less than 6X in this region on these two populations. SaltenE3 and E4 harbored an other close by SNP (transition C to T at position 80557). In order to evaluate how quick the two parallel SNPs at positions 80453 and 80495 became fixed within the evolved populations, we performed PCR amplification and sequencing of the locus at passage 1, 3 and 5 of the experimental evolution. A first parallel SNP (position 80495) were detected at the third but not the first passage of Salten's evolution. In fact, when looking at the raw data of the third passage, phages were able to infect the eight bacterial strains even though the ones allocated to ST319 showed incomplete inhibition of bacterial growth. When the second parallel SNP (position 80453) appeared at round five (ET5), the inhibition of bacterial growth of ST319 were almost complete phenotype.

However, most interestingly, in LTF_{pb1}, the two SNPs were non-synonymous as they replace an aline in valine at 1157 (Ala1157Val) and an asparagine in aspartic acid at 1178 (Asn1178Asp) (Fig.6F). Alanine and valine are quite similar, having an hydrophobic side chains with a longer chain in valine. Asparagine and aspartic acid belongs to different classes, as asparagine is polar uncharged and aspartic acid is negatively charged. On LTF_{pb1} structure (visualized on the 4UW7 PDB entry, from Garcia-Dorval, 2015), these mutations were located on external parts of the carboxy-terminal domain, pointing towards the curved groove at subunit interface, which was proposed to be the poly-mannose binding site of the protein (Fig.6E). Because the number of mutation was reduced, and given the importance of this protein in host-range specificity, the impact of these 2 SNPs on the phenotype were studied further in reverse-genetics.

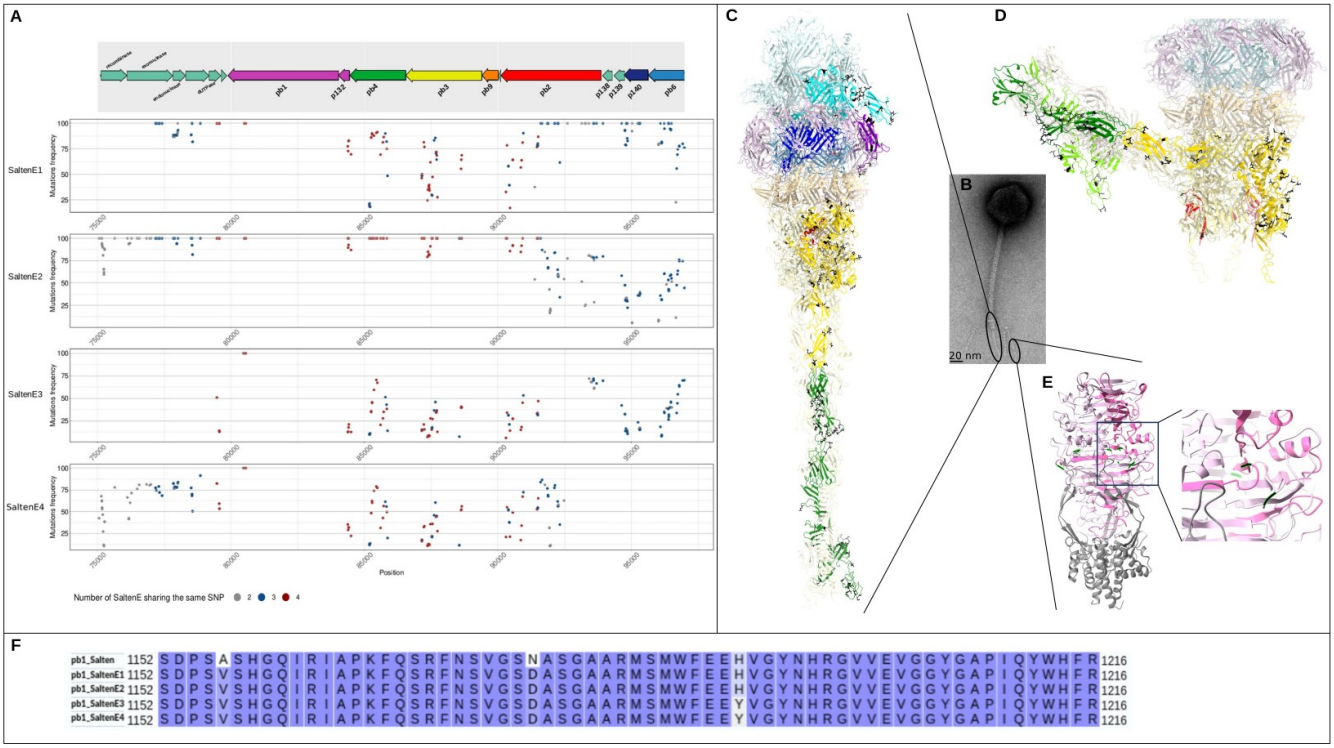

Figure 6. Parallel non-synonymous mutations visualization in the hot-spot of variation. A- Parallel non-synonymous mutations frequency according to their genomic position. Point-mutations in gray are shared by two lineages of evolved phages, in blue by three lineages and in dark red by all four lineages. **B,C,D,E-** Non-synonymous mutations representation on the T5 tail tip structure. B- Negative stain micrograph of phage T5. Ribbon representation of T5 tail tip structure before (C**-** 7ZHJ, 7ZQB) and after (D- 7ZN2, 7ZN4, 7ZQP) interaction with FhuA in nanodisc (Linares et al, 2023). E- Ribbon representation of the C-terminal tip of LTFpb1 with its chaperone domain (4UW8, Garcia-Dorval et la, 2015). Inset: blow up of the curved grooved proposed to be the poly-mannose binding site, here filled with a loop from the chaperone domain. In pb1, mutations are shown on the three subunits, for mutations pointing towards the curved groove belong to two different subunits. Only positions of mutations with weakly similar or dissimilar properties are displayed. In all panels, one monomer of each protein is coloured in a darker shade, the others, symmetry related proteins are coloured in a lighter shade of the same colour. For one monomer of each protein, the mutated residues are represented in black sticks and balls except for p140 in which they are red, and in pb1 in which they are black highlighted with green. Cyan: Tail Tube Protein pb6; blue: Baseplate Tail Tube Protein p140; purple: collar protein p132; orange: Distal Tail Protein pb9; gold: Baseplate Hub Protein pb3; green: Central Fiber Protein pb4, the three FNIII domains and the spike are in different shades of green; pink: lateral Long Tail Fiber pb1; grey: chaperone domain of pb1. **F-** Alignement of Salten and the four SaltenE of the 1152-1216 amino-acids zone, corresponding to the carboxy-terminal part of LTF_{pb1}. Visualization of two amino-acids substitutions shared by the four SaltenE (Ala1157Val and Asn1178Asp) at 100% and one (His1192Tyr) shared by SaltenE3 and SaltenE4.

Evaluation of point-mutations located in the LTF$_{pb1}$ on the phenotype

According to structural predictions (Fig 6E), the two LTF$_{pb1}$ mutations are predicted to be located on the binding site interface which interacts with the host surface. These two parallel mutations were thus good candidates to correspond to explain the phage adaptation to infect bacterial strains allocated to ST319. To directly demonstrate their effect on host-range expansion, we carried out a reverse-genetics experiment by introducing these two parallel mutations within the ancestral phage genome and creating a quasi-isogenic Salten phage mutant called « rE_Salten ». Applying the protocol described in Ramirez-Chamorro et al 2021 Front Microbiol, we took advantage of the natural high recombination rate of Tequintaviruses to transfer the two parallel mutation previously introduced within a plasmid. We thus inserted amplicons made from the evolved LTF$_{pb1}$ region into a plasmid that was subsequently introduced into the most susceptible bacterial strain SeeT17. After infection of this transformed SeeT17 by the ancestral phage population, we recovered the phage progeny and tested its phenotype on bacterial strains from ST319. In order to control for any biais introduced by this technic, we created two other transformed SeeT17: one in which we introduced an empty vector (rEV_Salten) and one in which we introduced a plasmid containing an insert made from amplicons made from the ancestral LTF$_{pb1}$ region (rA_Salten). If the two parallel mutation present in evolved phage populations were responsible for host-range expansion, we expected that bacterial strains from ST319 would become infected by rE_Salten but not rEV_Salten nor rA_Salten. As expected, the ancestral Salten as well as rEV_Salten and rA_Salten were not able to create clear lysis plaques on SeeT1, SeeT3, SeeT5 and SeeT6 (Fig 7A). The phenotype of inability of infection of SeeT5 and SeeT6 was obvious (no plaque observed) while these three phages were able to slightly infect SeeT1 and SeeT3 as they were able to form turbid lysis plaques. As expected, they were able to create clear lysis on SeeT17. Confirming our prediction, rE_Salten provoked clear lysis plaques on all bacterial strains (Fig 7A last column). We then verified the presence of the two parallel mutations within an isolated rE_Salten lysis plaque by sequencing amplicons targeting a large region of the LTFpb1 gene (larger than the plasmid insert). Additionally, to rule out a phenotype caused by an accidental contamination with an evolved phage, we sequenced a region of the gene coding for the TMP$_{pb2}$ harboring a specific signature of either the ancestral or evolved bacteriophages. This verification confirm that rE_Salten harbored the ancestral TMP$_{pb2}$.

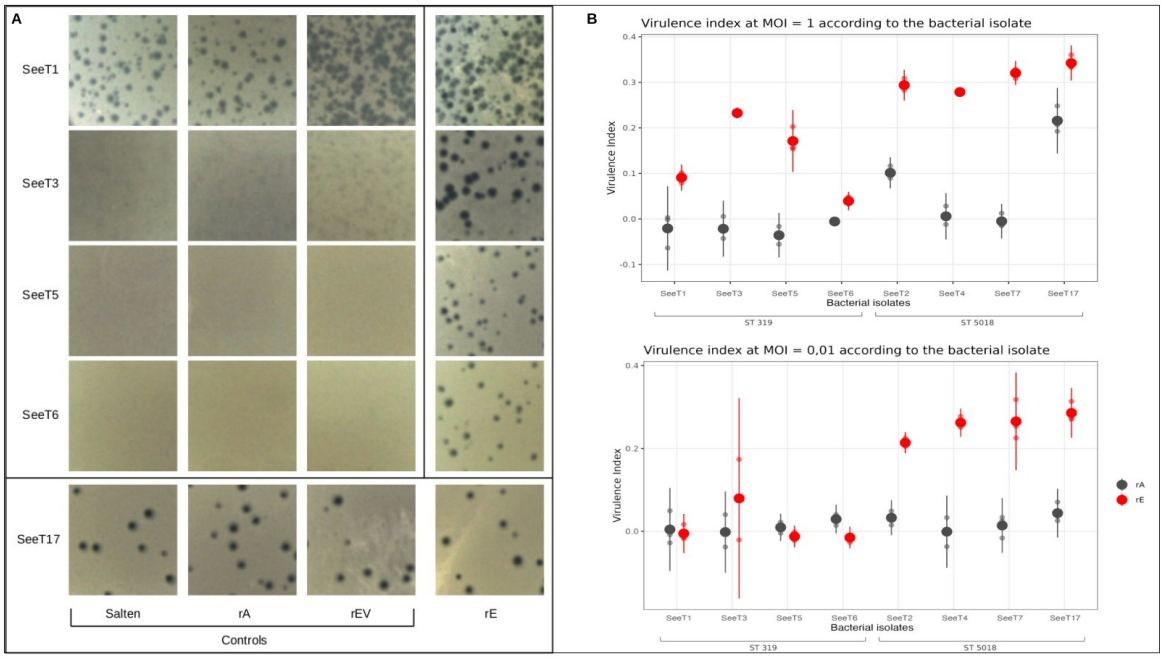

Figure 7. Host-range and virulence evaluation of rE_Salten. A- Visualization of the reverse-genetics double-layer assay. Bacteria are represented in rows and phages in columns. SeeT17 is a positive control as the ancestral Salten phage population is able to infect it well. rEV_Salten, rA_Salten and rE_Salten correspond to the ancestral phage having recombined with a plasmid harboring, respectively, no insert, an insert with the ancestral sequence of the LTF_{pb1} gene and finally the insert with the evolved sequence of the LTF_{pb1} gene. **B-** Virulence index (Vi) of rA_Salten (dark grey points) and rE_Salten (red points) according to *Salmonella enterica* genotypes and sequence types, at MOI = 1 (top graphic) and MOI = 0.01 (bottom graphic).

In order to evaluate if the two parallel mutations were also functional in liquid condition (i.e. the condition in which SaltenE evolved during our experiment), we compared the bacterial growth curves in presence of rA_Salten or rE_Salten at two multiplicities of infection (MOI = 0.01 and MOI =1). At high MOI, rE_Salten (emmean = 0.133 [0.122 - 0.145]) was indeed able to inhibit significantly more than rA_Salten (emmean = -0.021 [-0.032 - 0.010]) the growth of bacteria belonging to ST319 (Fig. 7B; posthoc contrast by pairs of phage; t_{30} = -20.214, p.value < 0.001). On the other hand, growth inhibition of bacteria belonging to ST319 in presence of rE_Salten and rA_Salten were not significantly different a low MOIs (t_{30} = -0.095, p.value = 0.925), indicating that the two parallel mutations were not involved in increasing virulence.

To conclude on this part, our results demonstrate that we identified the two adaptive mutations responsible for host-range expansion in our isolated *Tequintavirus*. Interestingly, these two mutations seem not to participate in a quantitative manner to an increase in virulence when infecting bacteria belonging to the resistant sequence type (ST319).

Discussion

The question on whether selection toward generalisation (i.e. ability to equivalently reproduce in different environments) evolve at the cost of lower mean fitness remains an open fundamental question (Bono et al., 2020; Sant et al., 2021) with applied consequences. For instance, in the field of bacterial control by phages, the use of cocktails composed by one generalist or several specialist phages does not lead to consensual answers across phage therapy experts (Rohde et al., 2018). In fact, using phages with low mean fitness might allow more cycles of bacterial reproduction leading to higher probabilities for resistant bacterial genotypes to appear (Oromí-Bosch et al., 2023; Betts et al., 2014; Friman et al., 2016; Zhang et al., 2021). Moreover, using several phages could modify phage-bacteria networks due to phage-phage (antagonistic) interactions (Molina et al., 2022; Jault et al., 2019).

To tackle this question, we designed an experimental evolution assay in order to expand from one to two sequence types (ST) a new *Tequintavirus* phage (called Salten) initially able to infect only one ST of *Salmonella enterica*. This experiment was repeated independently several times in the same conditions in order to reveal any convergent process that could be at work. Consistently, we were able to generate evolved phage populations (called SaltenE) harboring an expanded host-range and increased virulence. Analyses of genomic data of each evolved phage populations revealed the presence of hot-spots of mutations as well as mutations appearing at the same loci in several evolved phage populations (called parallel mutations), within genes coding for DNA modification or replication enzymes such as endonuclease, exonuclease, and Deoxyuridine 5'-triphosphate nucleotidohydrolase (dUTPase) as well as in caudal decorative domains. Interestingly, one parallel mutation appeared and fixed within the phage population earlier than any other ones and was one of the two parallel mutations accumulating within the long tail fiber (LTF_{pb1}) coding gene. We subsequently proved by reverse-genetics that these two mutations were directly involved in the host-range expansion.

Virus adaptation resides in optimizing the receptor use, translation machinery, assembly, horizontal transmission and bypass of cell defense (Simmonds et al., 2019). Not surprisingly, we observed first adaptive mutations accumulating within proteins involved in host recognition. In fact, genes coding for structural part represent a large part of phage genome (about 30%), which offers the possibility to mutations to accumulate at many loci. Previous results have shown that adaptive mutations impacted the host-interaction subunits proteins, such as capsides or spikes proteins for microvirid bacteriophages (Sackman et al., 2017), ΦX174 (Bull et al., 1997; Crill et al., 2000; Pepin et al., 2008) and receptor binding proteins in the RNA virus Φ6 (Duffy et al., 2006; Ferris et al., 2007) as well as almost hundred Caudoviricetes (Gaborieau et al., 2023). Interestingly, we didn’t observe any adaptive mutation in the gene coding for pb5 the major receptor binding proteins (RBP), that commits the phage to infection, triggering cell wall perforation and DNA ejection through a non-reversible interaction with FhuA, an outer-membrane ferrichrome transporter (Linares et al., 2023). Indeed, when looking carefully at

bacterial genome polymorphisms among the two sequence types (ST319 and ST5018), FhuA differed between STs by only two amino-acids located in the part inserted in the bacterial membrane with no extracellular interaction (Fig.S1C), that is without interaction with phage RBP (Degroux et al., 2023). Rather, we showed that mutations allowing host-range expansion were situated within the gene coding for LTF_{pb1}, a protein kwown to play an important role in host specificity (Heller & Braun, 1982; Heller, 1984) targeting O-antigens of lipopolysaccharides (LPS) involved in the first step of initial host recognition as well as related to reversible absorption (Golomidova et al., 2016; Sváb et al., 2018). More precisely, we showed that host-range mutations were situated in the C-terminal part of the long tail fiber (LTF_{pb1}), a region also involved in host-interaction of other morphotypic phages such as T3 (Yehl et al., 2019), T4 (Chen et al., 2017) and T7 (Sant et al., 2021; Yoichi et al., 2005). Strinkingly, our result are not in agreement with the only study on a *Tequintavirus* that reported that host interaction of LTF_{pb1} was situated in the N-terminal 400 base-pair region (Zhang et al., 2022). The discrepancy between our results might come from the fact that Zhang et al (2022) studied a LTF_{pb1} harboring a deletion in the C-terminal region in which Salten (our study) accumulated the two parallel mutations.

Beside the LTF_{pb1}, parallel mutations at the origin of non-synonymous amino-acids substitutions appeared interestingly in other caudal proteins that interact weakly with the surface membrane: TTP_{pb6}, p140, DTP_{pb9}, BHPB, pb4 and p132. In fact, these T5-like tail structural proteins are decorated with accessory domains or are composed of structural domains that either have protein or oligosaccharide binding folds and that have been proposed to increase phage infectivity by a specifically binding protein and/or saccharides at the surface of bacteria such as Ig-like domains including FNII domains (Fraser et al., 2007) or Oligosaccharide-binding domain (OB-Fold) (Breyton et al., 2013). A large part of the mutations being located on these « decorative » amino-acids interacting with the outside and the fact that the O-Ag seems to differ between STs, it looks like the phage has adapted in such a way as to optimize its first recognition of the host.

To partially conclude on this part, our results highlight temporal dynamic of adaptation of a T5-like virus. Indeed, we directly showed that the first mutation (Asn1179Asp in LTF_{pb1}) becoming fixed before any other adaptive mutation corresponds to a mutation involved in phage infection, most probably through recognition of host receptor. Interestingly, an other mutation (Ala1157Val) with weaker potential effect (but amino-acids harbor hydrophobic side chains) finally got fixed into LTF_{pb1} at the same time with other parallel mutations (i.e. after the fifth serial passage). Further studies might evaluate the effect of both mutations when alone, both on the stability of the LTF_{pb1} protein or the strength of interaction with LPS as well as host-range but also on bacterial growth inhibition. Finally, in order to evaluate to what extend the host-range has been expanded, further studies are needed to evaluate phenotypic effects of these host-range mutations on the ability to infect other genotypes of *Salmonella enterica* harboring some polymorphisms in the genes coding for LPS. Based on the fact that most host-range mutation have been shown to induce pleiotropic cost (Duffy et al., 2006), we expect that the two mutations reported in our study are specific to an environment composed of ST319 and ST5018 to which Salten

has been adapted to and would thus not contribute to infect bacterial genotypes harboring other LPS polymorphisms.

Compared with the actual literature, one striking result of our study resides in the fact that phage populations with expanded host-range didn't harbor any associated selective costs, since a significant increase in virulence was observed in evolved phage populations (Fig. 3A). What phenomenon could explain such discrepancy? If we consider the experimental evolution of ΦX174 where adaptation to *Salmonella enterica* was accompanied by a reduced ability to infect *Escherichia coli* (Crill et al., 2000), one of the difference (apart from the different genome size as well as the fact that ΦX174 evolved in chemostat) consisted in the fact that ΦX174 evolved in temporal variable environment while Salten evolved in spatial variable environment. Intuitively, we might expect that different type of mutations might be selected in according to temporal or spatial variable environments. In other words, organisms alternating between two environments (i.e. temporal variation) can accumulate mutations with selective cost since, at the same time, all competing organisms pay the same selective cost at the same time. Such phenomenon wouldn't apply in spatially variable environments since, at the same time (e.g. at each transfer), all organisms from the population are confronted to different environments. In spatially variable environments, natural selection would then select for mutations with the lowest selective costs.

Discrepancy between our results and the ones observed in Φ6 (Duffy et al., 2006; Ferris et al., 2007) might come from the fact that we let Salten evolve through several generations (six to seven serial passages) while virulence of host-range Φ6 mutants was measured after as few generation as possible, without letting compensatory mutation to accumulate. To test this hypothesis, we could propose to allow host-range Φ6 mutants to adapt to spatially variable environments composed of different bacterial host and we predict that other adaptive mutation would accumulate in other parts of the genome.

Finally, our results differ from the T7-like phage JB01 evolving on different strains of *E.coli* that also observed natural selection of low fitness generalist phage (Sant et al., 2021). We believe that two differences in our respective protocols may have caused our different results. First of all, we followed each phage-bacteria interaction with a spectrophotometer (measuring optical density) that allowed us to transfer any phage solution that presented even a slight inhibition effect on bacterial growth. We thus optimized the (hard) selection of infectious phages. Second, we applied the Appelmans protocol (Burrowes et al., 2019), that is we imposed a variations in multiplicities of infection (MOI) at each serial passage. Our protocol may thus have accelerated evolution compared to Sant's study. In fact, on the one hand, in solutions where MOI was high, we allowed both amphimixy and complementation to apply, that is favoring high diversity to be kept and exchanged among all phage genomes (Montville et al., 2005). On the other hand, in solutions where MOI was low, we allowed strong selection, removing any potentiality of phenotypic hiding of deleterious mutations (Novella et al., 2004; Froissart et al., 2004).

All these arguments may explain why we observed several parallel mutations, some of which (in LTF_{pb1}) we demonstrated to be directly involved in adaptation. Interestingly, some parallel mutations in non-structural genes might be responsible for the observed increased virulence, that is, the ability for phages to better reproduce within bacteria. Namely, we described in our study (Fig. 5A) the accumulation of parallel mutation within the deoxyuridine 5'-triphosphate nucleotidohydrolase (dUTPase) which is an enzyme at the origin of a phage counter-defense system. In fact, dUTPase allows to decrease uracil incorporation in new phage genomes and thus prevents cleavage of phage DNA by the Uracil DNA glycosylase (Ung) host enzyme which explains the fact that the less uracil is incorporated during phage replication, the more the phages multiply (Warner et al., 1979). Moreover, dUTPase action is facilitated by the action of early expression of phage T5.015 gene whose protein links to the bacterial Ung which blocks bacterial cell division and leads to bacteria death (Mahata et al., 2021). To test our hypothesis that parallel mutations observed in dUTPase participate to phage adaptation, we predict that, by integrating by reverse-genetics the mutated dUTPase into the ancestral phage genome, we shall observe an increased phage virulence after infection of bacteria of the two sequence types. To evaluate the generality of this mechanism of increase in virulence, we could compare the burst size of ancestral *versus* evolved phages mutated on their dUTPase after infection of other bacterial genotypes that would harbor variation in Ung protein.

The last striking result we would like to discuss deals with the high number of parallel mutations we observed. First of all, some of these parallel mutations can be explain by their presence at the beginning of the experiment but in very small quantities into secondary genomes spontaneously generated due to hyper-variable regions (Ig-like) or secondary genomes hitch-hiking with main genomes (while their modes of transmission need to be elucidated). Interestingly, other experimental evolution assays observed hundreds of parallel mutations such as with T7 (Bull et al., 2003) and we could propose the idea that our experiment selected a mutator genotype, a phenomenon proposed to be transient in conditions of changing environments (Mansky & Cunningham, 2000). Following this idea, our data showed parallel mutations in the related recombination exonuclease and the flap endonuclease (Fig 5A), two proteins orthologs to Mre11 - Rad50 (eukaryotes), SbcCD (prokaryotes), gp46/gp47 (phage T4) and gpD13/gpD12 (phage T5) (Rojowska, 2013) and localised near the DNA processing site (Käshammer et al., 2019). To test this hypothesis, we would further investigate the phage mutation rate in presence or absence of these parallel mutations but also further continue the serial passages, expecting that the mutator phenotype (if any) would revert after some time.

The last striking result we would like to discuss deals with the high number of parallel mutations we observed. Interestingly, other experimental evolution assays observed hundreds of parallel mutations such as with T7 (Bull et al., 2003). First of all, presence of some of these parallel mutations might be explained by their presence at the beginning of the experiment but in very few quantities into secondary genomes spontaneously generated in hyper-variable regions (Ig-like) or secondary genomes hitch-hiking with main genomes (while their modes of

transmission need to be elucidated). Second, such high number of mutations might be due to selection of mutator genotypes, a phenomenon proposed to be transiently adaptive in conditions of changing environments (Mansky & Cunningham, 2000). To support this hypothesis, some of the observed parallel mutations of SaltenE are present in the flap endonuclease and the recombination exonuclease, two proteins that have been proven to be involved in mutation rate variation, such as in myophage T4 (Mansky & Cunningham, 2000), podophage T7 (Tabor & Richardson, 1989) and SARS-CoV-2 (Amicone et al., 2022). Moreover, the similarity of Salten exonuclease with Rad50, a protein of the complex Mre11 - Rad50 (eukaryotes) which is known to be ortholog to SbcCD (prokaryotes), gp46/gp47 (phage T4) and gpD13/gpD12 (phage T5) (Rojowska, 2013), allowed us to localize parallel mutations near the DNA processing site (Käshammer et al., 2019). To test the mutator hypothesis, we would further investigate the phage mutation rate in presence or absence of these parallel mutations but also further continue the serial passages, expecting that the mutator phenotype (if any) would revert after some time.

Conclusion

Our study presents our ability to generate fairly rapidly (in six to eight days) new phages with high virulence and adapted to several bacterial genotypes that we choose *a priori*, a process that would be difficult to generate with synthetic biology despite its promises (Pirnay, 2020) . In fact, synthetic biology would target one or the other gene such as receptor binding proteins (Yehl et al., 2019) while we have shown here that compensatory mutations may appear in non expected proteins such as dUTPase or exonuclease. We believe that our results participate to the general understanding of phage genetic of adaptation and provide some insights on the complex adaptive walks phages are confronted to when facing spatially variable environment.

Author contribution

RF, AM conceived and designed the experiments. RF and AM performed the experiments with the help of CZ-C and MM-R for the reverse-genetics part and FXW for complete bacterial genome sequencing. RF, AM, MA, CB, SB, JH, JD, FXW, IB & AF analyzed the data. RF, AM, MA, XX, XX wrote the paper.

Aknowledgments

We thank M-S. Vernerey (PHIM) for the electron microscopy, C. Mariac (DIADE) for the library quality check before sequencing, A. Talman (MIVEGEC) for the help on the iSeq use, O. Rossier (UMR LPSE) for helpfull discussion on reverse-genetics, P. Agnew for his help on statistics, Y. Anciaux (ISEM) for the Vi calculation, J.

Garneau for PhageTerm help, M. Monot (I. Pasteur) and A. Dereeper (PHIM) for bioinformatic advices, and C. Torres-Barceló (INRAE), C. Whittington and XXX for helpfull commentary and discussion on the manuscript. The authors thanks UMR MIVEGEC for providing efficient environment and acknowledge the ISO 9001 certified IRD itrop HPC (member of the South Green Platform) and the whole bioinformatic team support in Montpellier for providing HPC resources that have contributed to the research results reported within this paper. URL: https://bioinfo.ird.fr/ - http://www.southgreen.fr This work was funded by Royal Canin through the support of the CNRS (contract 245420).

References

Abedon ST & Calendar R (2006) The Bacteriophages Oxford University Press, USA

Alikhan N-F, Zhou Z, Sergeant MJ & Achtman M (2018) A genomic overview of the population structure of Salmonella. PLOS Genetics 14: e1007261

Allen RC, Pfrunder-Cardozo KR, Meinel D, Egli A & Hall AR (2017) Associations among Antibiotic and Phage Resistance Phenotypes in Natural and Clinical Escherichia coli Isolates. mBio 8: 10.1128/mbio.01341-17

Amicone M, Borges V, Alves MJ, Isidro J, Zé-Zé L, Duarte S, Vieira L, Guiomar R, Gomes JP & Gordo I (2022) Mutation rate of SARS-CoV-2 and emergence of mutators during experimental evolution. Evolution, Medicine, and Public Health 10: 142-155

Aminov RI & Mackie RI (2007) Evolution and ecology of antibiotic resistance genes. FEMS Microbiology Letters 271: 147-161

Betts A, Kaltz O & Hochberg ME (2014) Contrasted coevolutionary dynamics between a bacterial pathogen and its bacteriophages. PNAS 111: 11109-11114

Bono LM, Draghi JA & Turner PE (2020) Evolvability Costs of Niche Expansion. Trends in Genetics 36: 14-23

Bono LM, Mao S, Done RE, Okamoto KW, Chan BK & Turner PE (2021) Chapter Three - Advancing phage therapy through the lens of virus host-breadth and emergence potential. In Advances in Virus Research, Kielian M Mettenleiter TC & Roossinck MJ (éd) p 63-110.

Breitbart M (2012) Marine Viruses: Truth or Dare. Annual Review of Marine Science 4: 425-448

Breyton C, Flayhan A, Gabel F, Lethier M, Durand G, Boulanger P, Chami M & Ebel C (2013) Assessing the Conformational Changes of pb5, the Receptor-binding Protein of Phage T5, upon Binding to Its Escherichia coli Receptor FhuA *. Journal of Biological Chemistry 288: 30763-30772

Brockhurst MA, Koskella B & Zhang Q-G (2017) Bacteria-Phage Antagonistic Coevolution and the Implications for Phage Therapy. In Bacteriophages: Biology, Technology, Therapy, Harper D Abedon S Burrowes B & McConville M (éd) p 1-21. Cham: Springer International Publishing Available at: https://doi.org/10.1007/978-3-319-40598-8_7-1

Bull JJ, Badgett MR, Rokyta D & Molineux IJ (2003) Experimental Evolution Yields Hundreds of Mutations in a Functional Viral Genome. J Mol Evol 57: 241-248

Bull JJ, Badgett MR, Wichman HA, Huelsenbeck JP, Hillis DM, Gulati A, Ho C & Molineux IJ (1997) Exceptional Convergent Evolution in a Virus. Genetics 147: 1497-1507

Burrowes BH, Molineux IJ & Fralick JA (2019) Directed in Vitro Evolution of Therapeutic Bacteriophages: The Appelmans Protocol. Viruses 11: 241

Chen M, Zhang L, Abdelgader SA, Yu L, Xu J, Yao H, Lu C & Zhang W (2017) Alterations in gp37 Expand the Host Range of a T4-Like Phage. Applied and Environmental Microbiology 83: e01576-17

Chevallereau A, Pons BJ, van Houte S & Westra ER (2022) Interactions between bacterial and phage communities in natural environments. Nat Rev Microbiol 20: 49-62

Crill WD, Wichman HA & Bull JJ (2000) Evolutionary Reversals During Viral Adaptation to Alternating Hosts. Genetics 154: 27-37

de Jonge PA, Nobrega FL, Brouns SJJ & Dutilh BE (2019) Molecular and Evolutionary Determinants of Bacteriophage Host Range. Trends in Microbiology 27: 51-63

Degroux S, Effantin G, Linares R, Schoehn G & Breyton C (2023) Deciphering Bacteriophage T5 Host Recognition Mechanism and Infection Trigger. Journal of Virology 97: e01584-22

Dion MB, Oechslin F & Moineau S (2020) Phage diversity, genomics and phylogeny. Nat Rev Microbiol 18: 125-138

Duerkop BA, Kleiner M, Paez-Espino D, Zhu W, Bushnell B, Hassell B, Winter SE, Kyrpides NC & Hooper LV (2018) Murine colitis reveals a disease-associated bacteriophage community. Nat Microbiol 3: 1023-1031

Duffy S, Turner PE & Burch CL (2006) Pleiotropic Costs of Niche Expansion in the RNA Bacteriophage Φ6. Genetics 172: 751-757

Egido JE, Costa AR, Aparicio-Maldonado C, Haas P-J & Brouns SJJ (2022) Mechanisms and clinical importance of bacteriophage resistance. FEMS Microbiology Reviews 46: fuab048

Ferris MT, Joyce P & Burch CL (2007) High Frequency of Mutations That Expand the Host Range of an RNA Virus. Genetics 176: 1013-1022

Fraser JS, Maxwell KL & Davidson AR (2007) Immunoglobulin-like domains on bacteriophage: weapons of modest damage? Current Opinion in Microbiology 10: 382-387

Friman V-P, Soanes-Brown D, Sierocinski P, Molin S, Johansen HK, Merabishvili M, Pirnay J-P, De Vos D & Buckling A (2016) Pre-adapting parasitic phages to a pathogen leads to increased pathogen clearance and lowered resistance evolution with Pseudomonas aeruginosa cystic fibrosis bacterial isolates. J Evol Biol 29: 188-198

Froissart R, Wilke CO, Montville R, Remold SK, Chao L & Turner PE (2004) Co-infection weakens selection against epistatic mutations in RNA viruses. Genetics 168: 9-19

Gaborieau B, Vaysset H, Tesson F, Charachon I, Dib N, Bernier J, Dequidt T, Georjon H, Clermont O, Hersen P, Debarbieux L, Ricard J-D, Denamur E & Bernheim A (2023) Predicting phage-bacteria interactions at

the strain level from genomes Microbiology Available at: http://biorxiv.org/lookup/doi/10.1101/2023.11.22.567924

Georjon H & Bernheim A (2023) The highly diverse antiphage defence systems of bacteria. Nat Rev Microbiol 21: 686-700

Golomidova AK, Kulikov EE, Prokhorov NS, Guerrero-Ferreira RC, Knirel YA, Kostryukova ES, Tarasyan KK & Letarov AV (2016) Branched Lateral Tail Fiber Organization in T5-Like Bacteriophages DT57C and DT571/2 is Revealed by Genetic and Functional Analysis. Viruses 8: 26

Heller K & Braun V (1982) Polymannose O-antigens of Escherichia coli, the binding sites for the reversible adsorption of bacteriophage T5+ via the L-shaped tail fibers. Journal of Virology 41: 222-227

Heller KJ (1984) Identification of the phage gene for host receptor specificity by analyzing hybrid phages of T5 and BF23. Virology 139: 11-21

Hyman P & Abedon ST (2010) Chapter 7 - Bacteriophage host range and bacterial resistance. Adv App Microbiol 70: 217-248

Jault P, Leclerc T, Jennes S, Pirnay JP, Que Y-A, Resch G, Rousseau AF, Ravat F, Carsin H, Le Floch R, Schaal JV, Soler C, Fevre C, Arnaud I, Bretaudeau L & Gabard J (2019) Efficacy and tolerability of a cocktail of bacteriophages to treat burn wounds infected by Pseudomonas aeruginosa (PhagoBurn): a randomised, controlled, double-blind phase 1/2 trial. Lancet Infect Dis 19: 35-45

Käshammer L, Saathoff J-H, Lammens K, Gut F, Bartho J, Alt A, Kessler B & Hopfner K-P (2019) Mechanism of DNA End Sensing and Processing by the Mre11-Rad50 Complex. Molecular Cell 76: 382-394.e6

Keen EC (2014) Tradeoffs in bacteriophage life histories. Bacteriophage 4: e28365

Kęsik-Szeloch A, Drulis-Kawa Z, Weber-Dąbrowska B, Kassner J, Majkowska-Skrobek G, Augustyniak D, Łusiak-Szelachowska M, Żaczek M, Górski A & Kropinski AM (2013) Characterising the biology of novel lytic bacteriophages infecting multidrug resistant Klebsiella pneumoniae. Virology Journal 10: 100

Koskella B & Meaden S (2013) Understanding Bacteriophage Specificity in Natural Microbial Communities. Viruses 5: 806-823

Leggett HC, Benmayor R, Hodgson DJ & Buckling A (2013) Experimental Evolution of Adaptive Phenotypic Plasticity in a Parasite. Current Biology 23: 139-142

Linares R, Arnaud C-A, Effantin G, Darnault C, Epalle NH, Boeri Erba E, Schoehn G & Breyton C (2023) Structural basis of bacteriophage T5 infection trigger and E. coli cell wall perforation. Science Advances 9: eade9674

Mahata T, Molshanski-Mor S, Goren MG, Jana B, Kohen-Manor M, Yosef I, Avram O, Pupko T, Salomon D & Qimron U (2021) A phage mechanism for selective nicking of dUMP-containing DNA. Proceedings of the National Academy of Sciences 118: e2026354118

Maiden MCJ, Bygraves JA, Feil E, Morelli G, Russell JE, Urwin R, Zhang Q, Zhou J, Zurth K, Caugant DA, Feavers IM, Achtman M & Spratt BG (1998) Multilocus sequence typing: A portable approach to the identification of clones within populations of pathogenic microorganisms. Proceedings of the National Academy of Sciences 95: 3140-3145

Mansky LM & Cunningham KS (2000) Virus mutators and antimutators: roles in evolution, pathogenesis and emergence. Trends in Genetics 16: 512-517

Mathieu A, Dion M, Deng L, Tremblay D, Moncaut E, Shah SA, Stokholm J, Krogfelt KA, Schjørring S, Bisgaard H, Nielsen DS, Moineau S & Petit M-A (2020) Virulent coliphages in 1-year-old children fecal samples are fewer, but more infectious than temperate coliphages. Nat Commun 11: 378

Meaden S & Koskella B (2013) Exploring the risks of phage application in the environment. Front Microbiol 4 Available at: http://www.ncbi.nlm.nih.gov/pmc/articles/PMC3843224/

Molina F, Menor-Flores M, Fernández L, Vega-Rodríguez MA & García P (2022) Systematic analysis of putative phage-phage interactions on minimum-sized phage cocktails. Sci Rep 12: 2458

Montville R, Froissart R, Remold SK, Tenaillon O & Turner PE (2005) Evolution of mutational robustness in an RNA virus. PLoS Biol. 3: e381

Nobrega FL, Vlot M, de Jonge PA, Dreesens LL, Beaumont HJE, Lavigne R, Dutilh BE & Brouns SJJ (2018) Targeting mechanisms of tailed bacteriophages. Nat Rev Microbiol 16: 760-773

Norman JM, Handley SA, Baldridge MT, Droit L, Liu CY, Keller BC, Kambal A, Monaco CL, Zhao G, Fleshner P, Stappenbeck TS, McGovern DPB, Keshavarzian A, Mutlu EA, Sauk J, Gevers D, Xavier RJ, Wang D, Parkes M & Virgin HW (2015) Disease-Specific Alterations in the Enteric Virome in Inflammatory Bowel Disease. Cell 160: 447-460

Novella IS, Reissig DD & Wilke CO (2004) Density-dependent selection in vesicular stomatitis virus. J Virol 78: 5799-804

Oromí-Bosch A, Antani JD & Turner PE (2023) Developing Phage Therapy That Overcomes the Evolution of Bacterial Resistance. Annual Review of Virology 10: 503-524

Pepin KM, Domsic J & McKenna R (2008) Genomic evolution in a virus under specific selection for host recognition. Infection, Genetics and Evolution 8: 825-834

Pirnay J-P (2020) Phage Therapy in the Year 2035. Front. Microbiol. 11: 1171

Reyes A, Haynes M, Hanson N, Angly FE, Heath AC, Rohwer F & Gordon JI (2010) Viruses in the faecal microbiota of monozygotic twins and their mothers. Nature 466: 334-338

Rohde C, Resch G, Pirnay J-P, Blasdel BG, Debarbieux L, Gelman D, Górski A, Hazan R, Huys I, Kakabadze E, Łobocka M, Maestri A, Almeida GM de F, Makalatia K, Malik DJ, Mašlaňová I, Merabishvili M, Pantucek R, Rose T, Štveráková D, et al. (2018) Expert Opinion on Three Phage Therapy Related Topics: Bacterial Phage Resistance, Phage Training and Prophages in Bacterial Production Strains. Viruses 10: 178

Rojowska AM (2013) Structural and functional analysis of DNA binding by the Rad50 catalytic head from Thermotoga maritima.

Roux S & Emerson JB (2022) Diversity in the soil virosphere: to infinity and beyond? Trends in Microbiology 30: 1025-1035

Sackman AM, McGee LW, Morrison AJ, Pierce J, Anisman J, Hamilton H, Sanderbeck S, Newman C & Rokyta DR (2017) Mutation-Driven Parallel Evolution during Viral Adaptation. Molecular Biology and Evolution 34: 3243-3253

Sant DG, Woods LC, Barr JJ & McDonald MJ (2021) Host diversity slows bacteriophage adaptation by selecting generalists over specialists. Nat Ecol Evol 5: 350-359

Simmonds P, Aiewsakun P & Katzourakis A (2019) Prisoners of war — host adaptation and its constraints on virus evolution. Nat Rev Microbiol 17: 321-328

Storz JF (2016) Causes of molecular convergence and parallelism in protein evolution. Nat Rev Genet 17: 239-250

Suttle CA (2007) Marine viruses — major players in the global ecosystem. Nat Rev Microbiol 5: 801-812

Sváb D, Falgenhauer L, Rohde M, Szabó J, Chakraborty T & Tóth I (2018) Identification and Characterization of T5-Like Bacteriophages Representing Two Novel Subgroups from Food Products. Frontiers in Microbiology 9 Available at: https://www.frontiersin.org/journals/microbiology/articles/10.3389/fmicb.2018.00202

Tabor S & Richardson CC (1989) Selective Inactivation of the Exonuclease Activity of Bacteriophage T7 DNA Polymerase by in Vitro Mutagenesis. Journal of Biological Chemistry 264: 6447-6458

Tesson F, Hervé A, Mordret E, Touchon M, d'Humières C, Cury J & Bernheim A (2022) Systematic and quantitative view of the antiviral arsenal of prokaryotes. Nat Commun 13: 2561

Warner HR, Thompson RB, Mozer TJ & Duncan BK (1979) The properties of a bacteriophage T5 mutant unable to induce deoxyuridine 5'-triphosphate nucleotidohydrolase. Synthesis of uracil-containing T5 deoxyribonucleic acid. Journal of Biological Chemistry 254: 7534-7539

Woolhouse MEJ, Taylor LH & Haydon DT (2001) Population Biology of Multihost Pathogens. Science 292: 1109-1112

Yehl K, Lemire S, Yang AC, Ando H, Mimee M, Torres MDT, De La Fuente-Nunez C & Lu TK (2019) Engineering Phage Host-Range and Suppressing Bacterial Resistance through Phage Tail Fiber Mutagenesis. Cell 179: 459-469.e9

Yoichi M, Abe M, Miyanaga K, Unno H & Tanji Y (2005) Alteration of tail fiber protein gp38 enables T2 phage to infect Escherichia coli O157:H7. Journal of Biotechnology 115: 101-107

Zhang J, Ning H, Lin H, She J, Wang L, Jing Y & Wang J (2022) Expansion of the Plaquing Host Range and Improvement of the Absorption Rate of a T5-like Salmonella Phage by Altering the Long Tail Fibers. Applied and Environmental Microbiology 0: e00895-22

Zhang Q-G, Chu X-L & Buckling A (2021) Overcoming the growth–infectivity trade-off in a bacteriophage slows bacterial resistance evolution. Evolutionary Applications 14: 2055-2063

Zhou Z, Alikhan N-F, Mohamed K, Fan Y & Achtman M (2020) The EnteroBase user's guide, with case studies on Salmonella transmissions, Yersinia pestis phylogeny, and Escherichia core genomic diversity. Genome Res 30: 138-152

Supplementary Figures and Tables

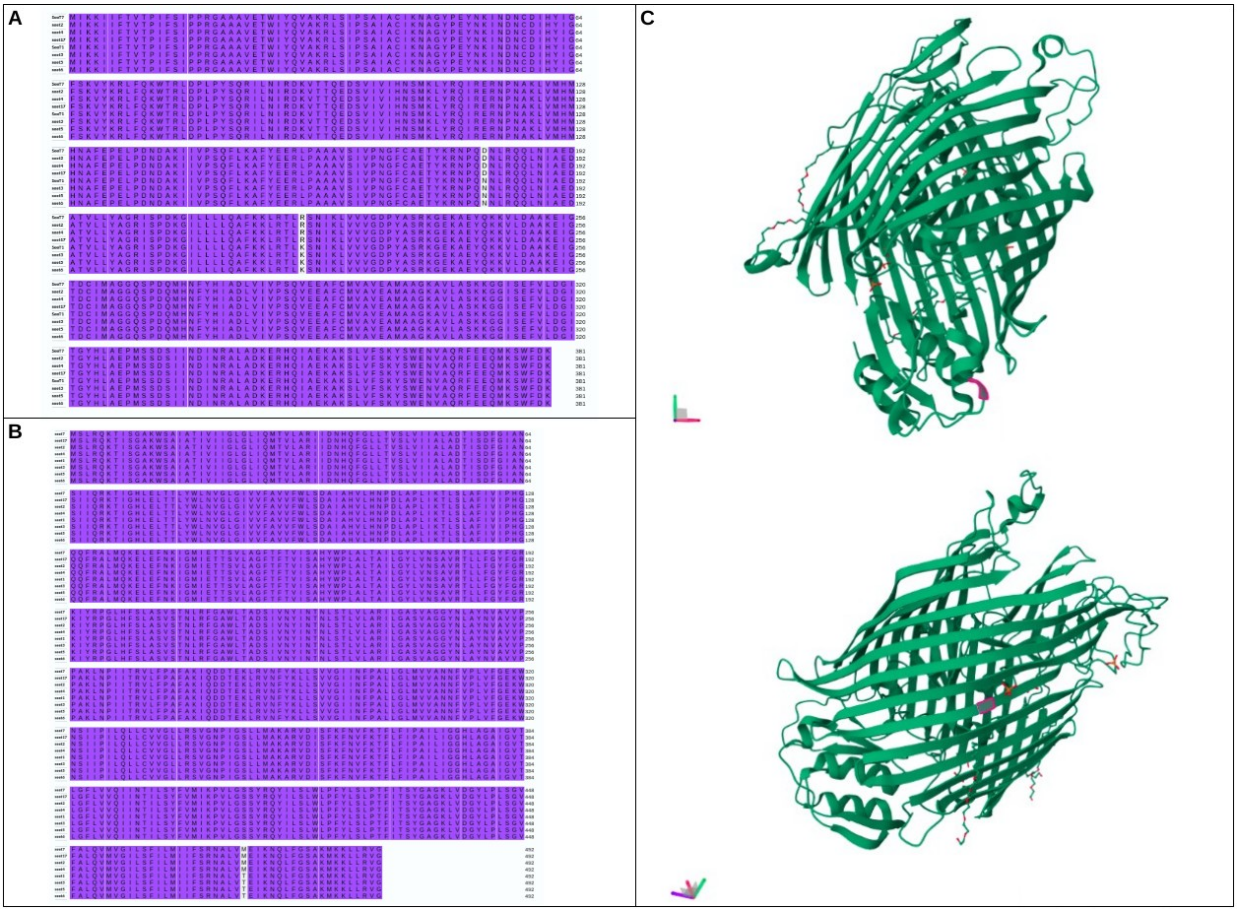

Figure S1. Receptors genetic diversity. A- Alignment on Uniprot of the waaK gene retrieved in each genome of the height bacterial isolates SeeT used for the evolutionary training. **B-** Alignment on Uniprot of the wzxC gene retrieved in each genome of the height bacterial isolates SeeT used for the evolutionary training. **C-** FhuA : visualization of the Ser50Ala position (top) and Glu368Ala position (bottom) on the 3D ribbon representation of PDB 2W16.

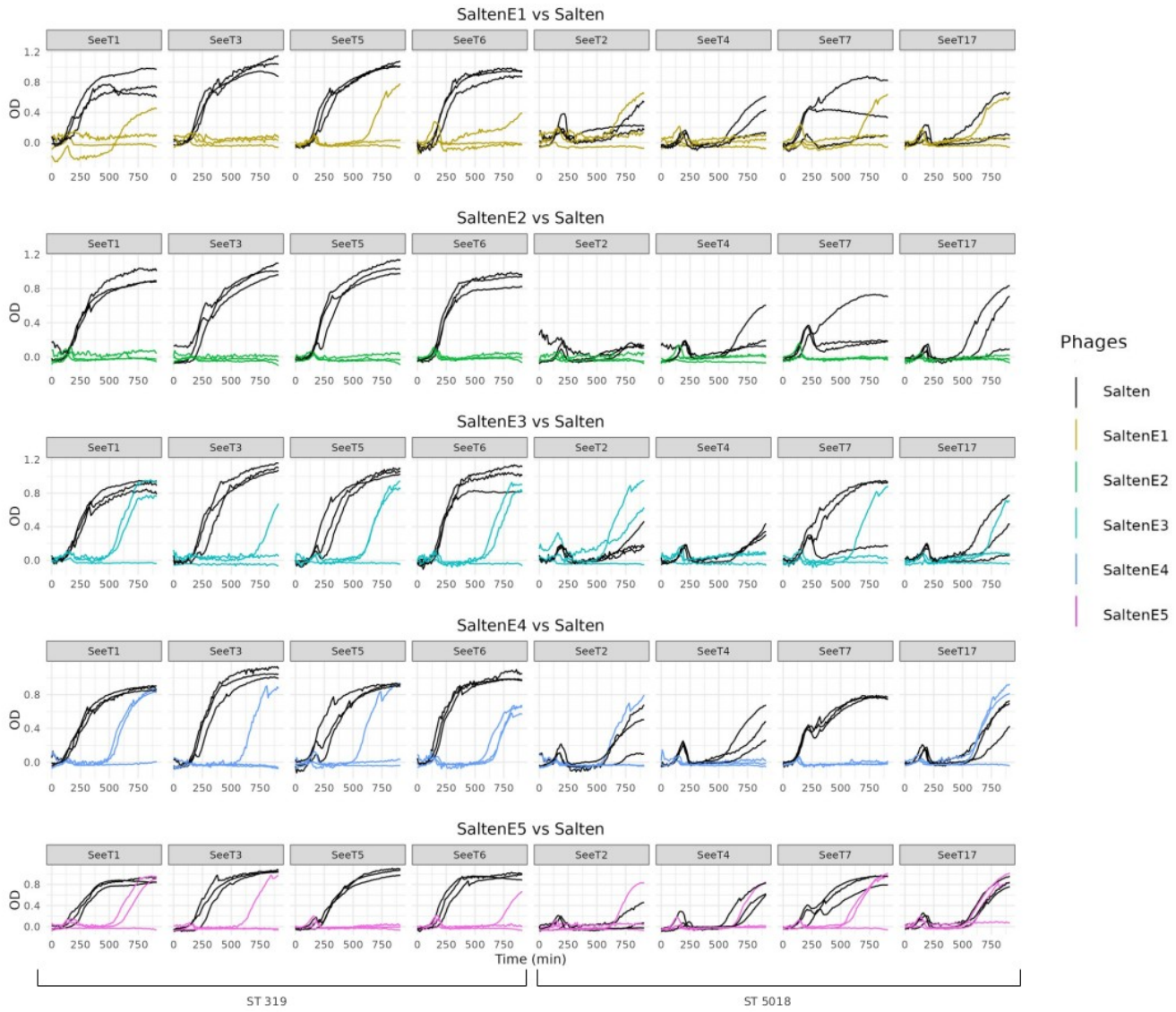

Figure S2. Kinetics of bacterial growth (OD) according to the time (min) in presence of ancestral (black) or experimentally evolved (colored) bacteriophages. Each phage was tested three biological independent times against each of the eight bacterial isolates used during the experimental evolution.

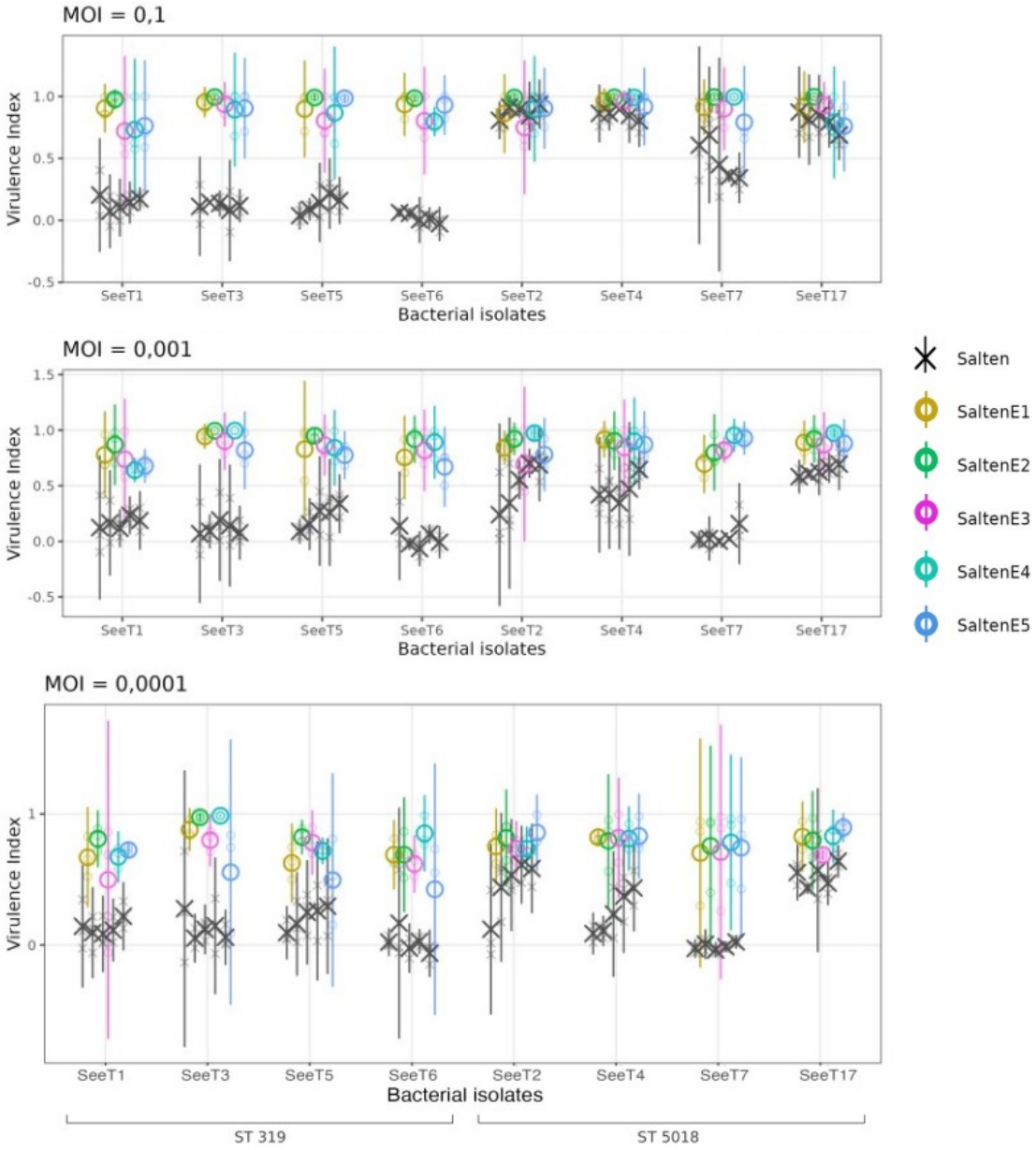

Figure S3. Bacteriophage virulence index at different MOI. Evaluation of the bacteriophage virulence index at MOI=0.1, MOI=0.001 and MOI=0.0001 according to the eight SeeTs grown in liquid cultures in presence of Salten(black cross) or SaltenE lineages (colored circles) . SeeT's genotypes are divided according to their ST.

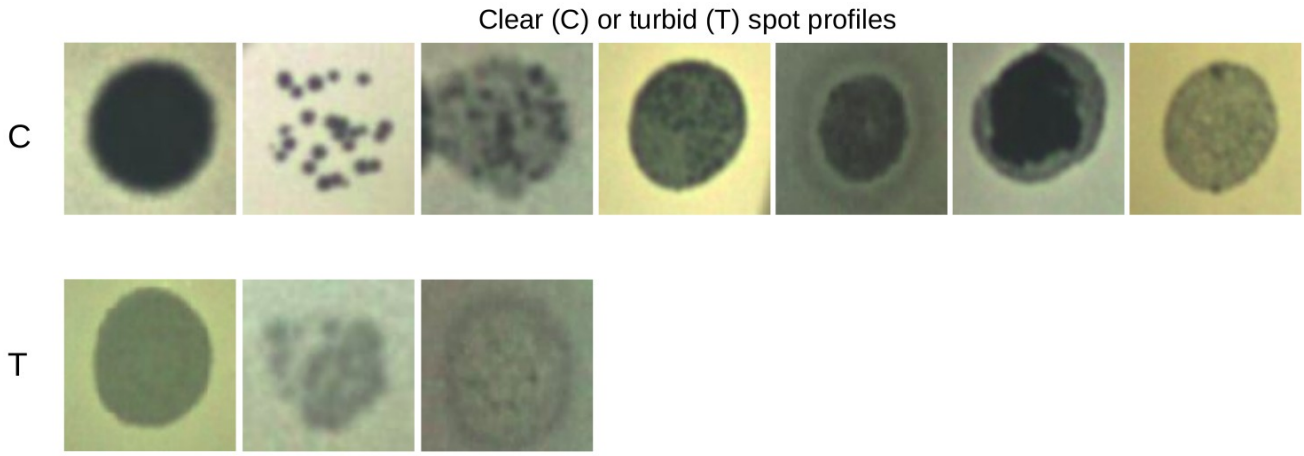

Figure S4. Exemple of spot profiles that have been classified as clear or turbid. C = exemples of plaques profile associated to clear phenotype. T = exemples of plaques associated to turbid phenotype.

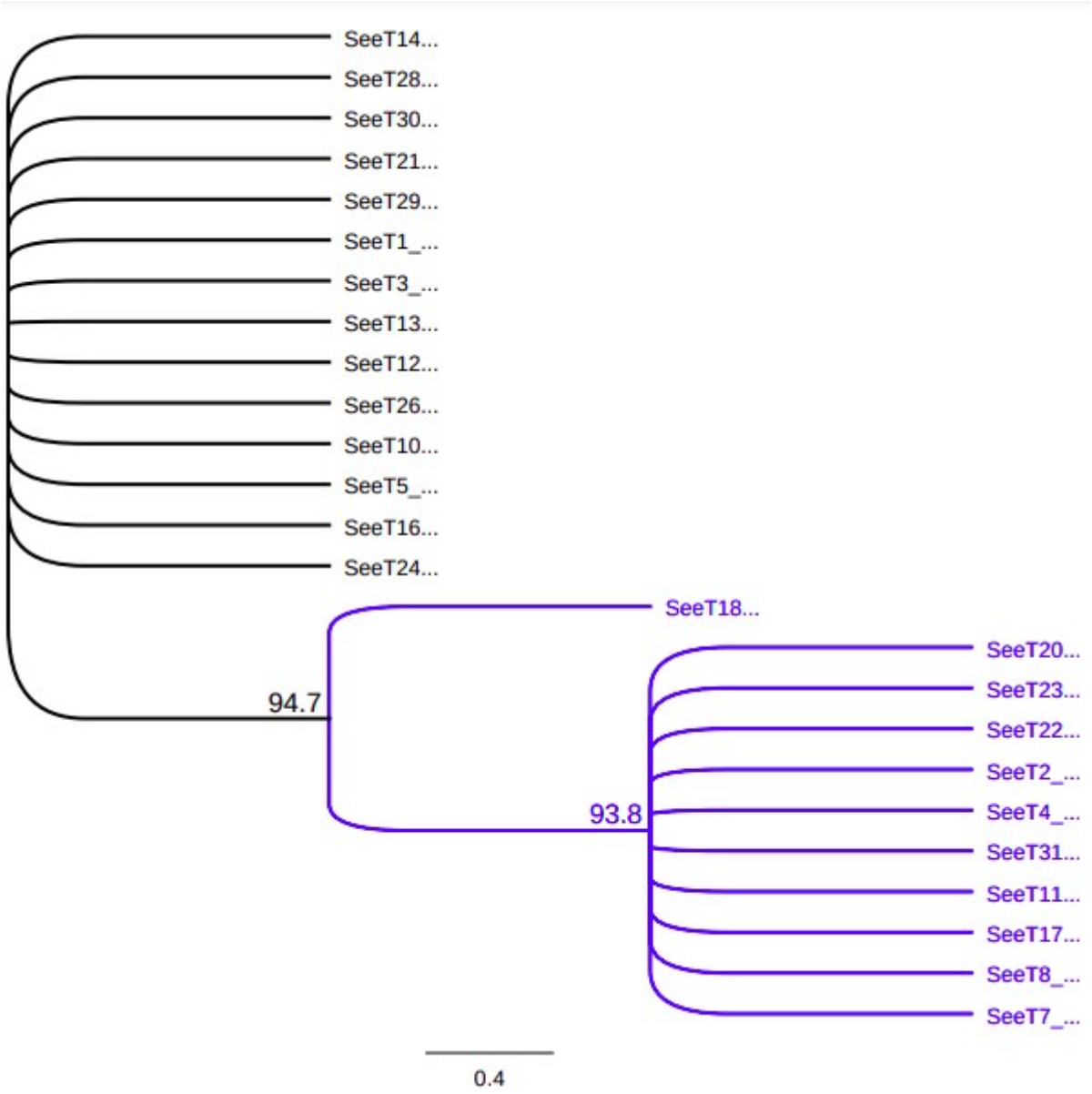

Figure S5. Phylogenetic tree based on the genetic distance of cpn60 gene between the 26 SeeTs.

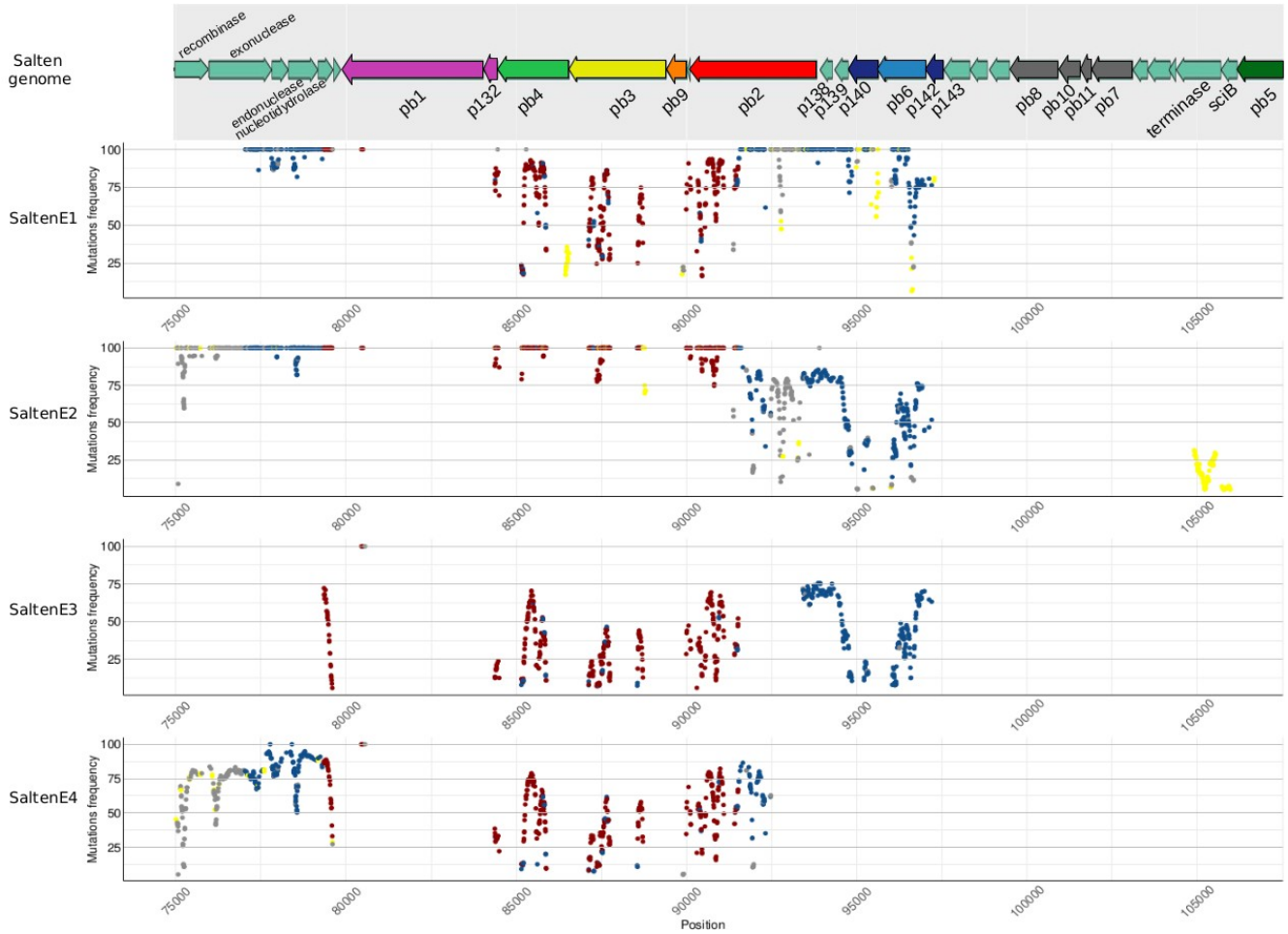

Figure S6. Visualization of point-mutations and their location concerning four evolved phage population SalteE in a hot-spot of mutations between 75kb and 100kb. On the top, genomic map of the ancestral phage Salten to locate mutations positions. This part of the genome corresponds to genes coding enzymes that modify DNA and structural genes coding tail fibers. Mutations frequency of point-mutations (colored points) for each evolved phages population, according to their position. Point-mutations in yellow are only present on one evolved phage lineage. Point-mutations in gray are shared by two lineages, in blue by three lineages and in dark red by all four lineages.

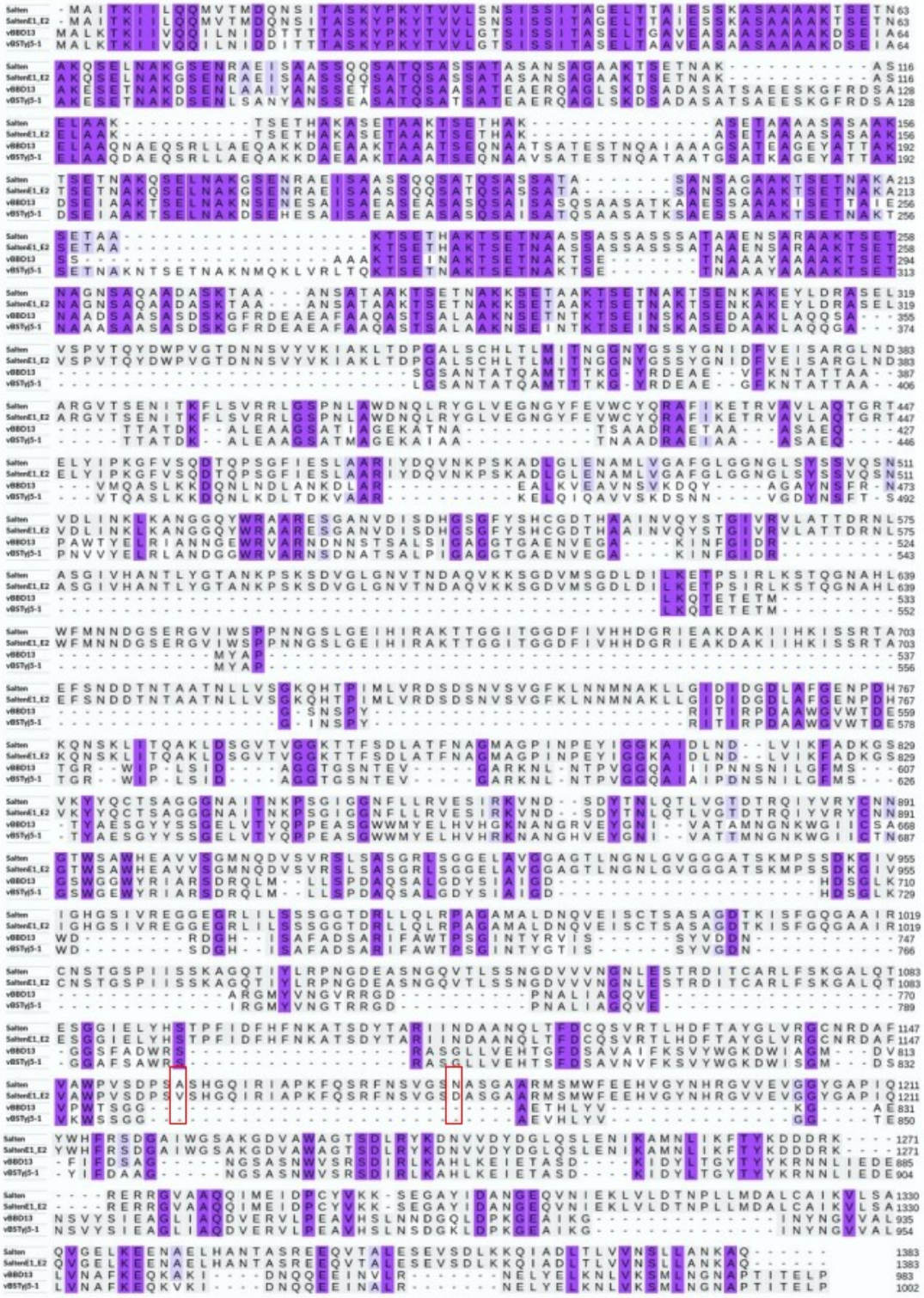

Figure S7. Alignment of Long Tail Fiber amino-acids sequences of Salten, SaltenE1/E2, vB BD13 and vB STyj5-1 from Zhang et al (2022). The two amino-acids substitutions found in SaltenE phages populations are highlighted with a red rectangle. vB BD13 and vB STyj5-1 phages from Zhang et al are lacking the locus containing SaltenE's mutations.

TableS1

Usage	Oligo Name	Sequence (5’>3’)
pBBR1-MSC2 construction	Salten-pb1-3374-F	aaaaggtctcattttAAAGTGTGCGCACATTGCAT
Phylogeny on all SeeTs	M13_cpn60_F	cgccagggttttcccagtcacgacGAIIIIGCIGGIGAYGGIACIACIAC
Phylogeny on all SeeTs	M13_cpn60_R	agcggataacaatttcacacaggaYKIYKITCICCRAAICCIGGIGCYTT
pBBR1-MSC2 construction	Salten-pb1-3557-R	aaaaggtctcaggggGACATCCTTGCAGCTCCAGA
Presence of insert	pBBR1-MSC2-F	TGCGCAACTGTTGGGAAG
Presence of insert	Salten-pb1-3470-F	aaaaggtctcattttGTCTGTCAGCCATGGTCAGA
Presence of mutations and order of mutations arrival	Salten-pb1-3183-F	AGGCATCGAATGGTCAGGTG
Presence of mutations and order of mutations arrival	Salten-pb1-4136-R	CTAGGGCTGTGACTTGCTCC
Verification of phage contamination and order of mutations arrival	Salten-pb2-8720-F	GCAACCCGTACTGCAAAGTC
Verification of phage contamination and order of mutations arrival	Salten-pb2-9129-R	GCGGCACCAGCAGTATCAT
Order of mutations arrival	Salten-753-exonuc-F	AGCTGTACAAGTTGCCGAAC
Order of mutations arrival	Salten-1198-exonuc-R	GTTGTCGGATTTGCACCTGT